The Thesis Committee for Kelly Elizabeth Hattori
Certifies that this is the approved version of the following thesis:

Architecture of a mid-Cretaceous patch reef: High resolution mapping provides new insight into facies geometries and ecological relationships at Paul Spur, Bisbee, Arizona.

APPROVED BY
SUPERVISING COMMITTEE:

Supervisor: _____
Rowan C. Martindale

Co-Supervisor: _____
Charles Kerans

_____
Ann M. Molineux

Architecture of a mid-Cretaceous patch reef: High resolution mapping provides new insight into facies geometries and ecological relationships at Paul Spur, Bisbee, Arizona.

by

Kelly Elizabeth Hattori, B.S.

Thesis

Presented to the Faculty of the Graduate School of

The University of Texas at Austin

in Partial Fulfillment

of the Requirements

for the Degree of

Master of Science in Geological Sciences

The University of Texas at Austin

May 2017

Dedication

To my parents, Dave and Lori, for their endless love and support and for always being my biggest cheerleaders. And to all of my friends, for always putting up with my rants on rocks and the silliness of my everyday life as a graduate student.

Acknowledgements

This master's research was funded through generous grants from the Association for Women Geoscientists, the Evolving Earth Foundation, the Geological Society of America, the Lerner-Gray Memorial Fund (managed by the American Museum of Natural History), the Paleontological Society, and the Jackson School of Geosciences at the University of Texas at Austin.

I would like to thank my advisors, Dr. Charles Kerans and Dr. Rowan Martindale, for their guidance and insight. Their expertise was instrumental in helping me turn my thesis into a project that has applications in both the realm of paleontology and carbonate geology. This study benefited greatly from the knowledge of committee members Dr. Charles Kerans, Dr. Ann Molineux, and Dr. Rowan Martindale, whose comments and edits helped to focus this manuscript into a better, more targeted study. I would also like to thank the members of the Reservoir Characterization Research Laboratory for their incredibly helpful guidance and insight, for allowing me to use their equipment, and for always being up for a good discussion. Without your support, I would be a lesser geologist and this research would not have been possible.

Finally, I would like to thank my field assistants Elizabeth Reinthal, Nicholas Ettinger, Benjamin Smith, and Chiara Tornabene for their help out at Paul Spur. Together, we braved rattlesnakes, border patrol, helicopter flyovers, swarms of bees, and sketchy situations in the quest to understand the history of a Cretaceous reef. You all are awesome!

Abstract

Architecture of a mid-Cretaceous patch reef: High resolution mapping provides new insight into facies geometries and ecological relationships at Paul Spur, Bisbee, Arizona.

Kelly Elizabeth Hattori, M.S. Geo. Sci.

The University of Texas at Austin, 2017

Supervisors: Rowan Martindale and Charles Kerans

Patch reef complexes are commonly found in the shelf interior of carbonate platforms. These small scattered buildups are potential hydrocarbon targets in the Maverick Basin and more broadly within Cretaceous reservoirs in the Middle East. The three-dimensional facies architecture within patch reefs is difficult to determine using only subsurface data. Lateral facies distribution and overall patch reef architecture is better assessed in outcrop analogs.

The Paul Spur patch reefs near Bisbee, Arizona are ideally suited for assessing three-dimensional spatial and temporal facies variability. Previous interpretations of this 1.5 km-long exposure of Mural Limestone disagree as to the overall history of the reef with regards to facies relationships and distribution. Early work at Paul Spur attributed spatial facies distribution to biotic zonation of a reef during one period of growth, while later work concluded that it preserves multiple stages of reef growth with facies succession and variation both spatially and temporally controlled.

This work better resolves the depositional history and biotic composition of the Paul Spur patch reef complex with respect to stratal geometry and both spatial and temporal facies relationships. High-resolution lateral facies mapping of the exposed reef top is integrated with three-dimensional digital outcrop modeling techniques to facilitate improved understanding of the history of reef growth and patch reef architecture. The new reef architecture interpretations are integrated into the preexisting depositional model. At Paul Spur, multiple stages of reef growth are preserved and exhibit variable architectures controlled largely by local sea-level fluctuations and sediment influx. While coral diversity increases throughout the depositional history of the reef complex, overall abundance decreases as rudists become more common, reflecting an evolution of the reef community through time. Reef constituents are heterogeneously distributed within facies, highlighting the need for careful analysis and outcrop scale synthesis of the paleoecological data to avoid erroneous characterization of depositional environments based solely on the organisms found within a small area. The new depositional model developed in this study improves the utility of Paul Spur as an outcrop analog for patch reefs identified in the subsurface and furthers understanding of the relationship between environmental controls and reef development.

Table of Contents

List of Tables

List of Figures

Chapter 1: Introduction

During the Cretaceous Period, shallow-water reefs in the Tethys Ocean were dynamic communities with constantly shifting biotic compositions and diversities. In the earliest Cretaceous, reefs were dominated by scleractinian corals; as the period progressed, a group of heterodontid bivalves called rudists (Order Hippuritida Newell, 1965) (Skelton, 2013) also took on a reef-building role. These bivalves, which first appeared in the late Jurassic (Oxfordian), repeatedly rose to prominence as major reef-builders in the Cretaceous, completely dominating reefs in some Tethyan regions at times and experiencing heavy decline or extinction during others and ultimately going completely extinct in the end-Cretaceous mass extinction (Scott, 1995).

Mid-Cretaceous reefs from North America have been extensively studied and generally exhibit a vertical progression from initially coral-dominated reef frameworks to rudist-dominated assemblages (e.g. Scott and Brenckle, 1977; Scott, 1984, 1988; Scott et al., 1990; Aisner, 2010). Previous work has attributed the change in biotic composition and turnover mainly to competition between corals and rudists (Kauffman and Johnson, 1988; Johnson, 2002) and biotic zonation based on water depth (Scott and Brenckle, 1977; Roybal, 1981; Scott, 1979, 1984, 1988, 1995; Scott et al., 1990). The latter, more popular hypothesis typically relies on fluctuations in eustatic sea level as a mechanism for the observed faunal turnover. Rudists are thought to have lived in shallow-water habitats above fair weather wave base in areas of higher wave energy and may have flourished in warmer, more saline waters (Roybal, 1981; Scott, 1988; Johnson et al., 1996; Johnson, 2002). In contrast, corals are thought to have colonized deeper, calmer, cooler waters (Scott, 1988, 1995; Scott et al., 1990). Rather than directly outcompeting corals, it was hypothesized that

rudists simply filled empty niche spaces as the less robust corals declined or moved into deeper, cooler waters.

The spread of rudists may have been mediated by fluctuations in sea level or environmental perturbations such as oceanic anoxic events (OAEs). For example, a decrease in sea level could reduce habitable area, and could cause subaerial exposure as well as increase salinity and temperatures above thresholds that even rudists could tolerate (Jenkyns, 1980). Two major declines in rudist diversity and abundance coincide with or are closely associated with OAEs 1a and 2 in the early Aptian and at the Cenomanian-Turonian boundary, respectively (Scott, 1995; Skelton and Gili, 2012). During periods following rudist decline and extinction, corals rose to prominence as dominant framework builders on reefs, but declined again when rudists began to recover and proliferate. Thus, reefs built just after major perturbations can provide insight into dynamics between corals and rudists, particularly with respect to rudist re-colonization and coral response to their reappearance.

Mid-Cretaceous (late Aptian to early Albian) reefs are ideal for studying reef recovery and community development through time. By the late Early Cretaceous, rudists had developed different morphotypes suited for a variety of roles within a reef ecosystem; recumbent rudists nestled in the substrate or into sheltered areas, while elevator rudists stood erect and may have protruded upwards into the water column (Skelton, 1978). Differences in morphotypes aid in the determination of the role of rudists during different stages of reef development. Analysis of the progression of post-OAE recovery faunas in shallow water tropical reefs could, therefore, be the key to understanding the relationship between corals and rudists as major framework-building reef constituents.

This study utilizes high-resolution comprehensive mapping data for an outcrop of the extreme northwest embayment of the Chihuahua Trough of the Gulf of Mexico, known

as Paul Spur, to investigate the development of a post-perturbation Aptian-Albian patch reef of the Mural Limestone of Arizona. The goal of this work is to assess community recovery and transitions, zonation, and facies architecture of the reef, and to reassess the stratigraphic framework currently in place using advanced three-dimensional digital techniques. Aerial imagery of the outcrop captured by an unmanned aerial vehicle (UAV) is processed into a photogrammetric three-dimensional model of the outcrop and facilitates improved understanding of the history of reef growth and overall patch reef architecture. Integration of the three-dimensional model with detailed facies mapping provides a high-resolution view of reef development that is useful for predicting the architecture of subsurface patch reefs of similar composition and history. Here, we also investigate the validity of perturbations, such as pulsed anoxia during OAE 1b or fluctuations in sea level, as a mechanism influencing development of the Paul Spur reef with respect to community recovery and ecological transitions. Additionally, the study aims to address the likelihood of competition-mediated or environmentally-mediated population dynamics between rudists and corals.

Chapter 2: Geologic Setting

The present study focuses on Paul Spur, an outcrop of Upper Mural Limestone preserving a patch reef complex located southeast of Bisbee, Arizona, USA, on Highway 80 (Fig. 1). The complex is composed of a series of patch reefs with distinct windward (southeast) to leeward (northwest) asymmetry; successive stages of the reef backstep to the north (Aisner, 2010). The outcrop is exposed in a northwest- to southeast-trending synclinal fold produced by the Laramide orogeny in the Late Cretaceous (Hayes, 1970).

STRATIGRAPHY

The Mural Limestone is an early Albian formation within the Bisbee Group that represents the shelf of a distally-steepened ramp that prograded into the Chihuahua Trough (Fig. 2). The deposition of Mural carbonates succeeding siliciclastics of the Morita Formation began in the latest early Aptian during a period of sea level rise and ended in the middle Albian with another episode of sea level rise accompanied by burial by clastic sediments of the Cintura Formation (Fig. 3) (Scott, 1987; Warzeski, 1987; Scott and Warzeski, 1993). The Mural Limestone encompasses a large-scale transgressive-regressive sequence and was originally divided into two members: the transgressive Lower Mural and the regressive aggradational-progradational Upper Mural (Warzeski, 1987; Scott and Warzeski, 1993), which are divided by a late Aptian maximum flooding surface defined by Scott (1987). In southeastern Arizona, the Upper Mural is exposed as a series of shelf carbonates, patch reefs, and high-energy shoals; in Sonora, Mexico, it is composed of large patch reefs and sand banks that may represent the early stages of development of a platform margin (Scott and Warzeski, 1993). Aisner (2010) noted that though Paul Spur is within the reefal region of the Upper Mural, it is likely within a transgressive sequence; the Upper

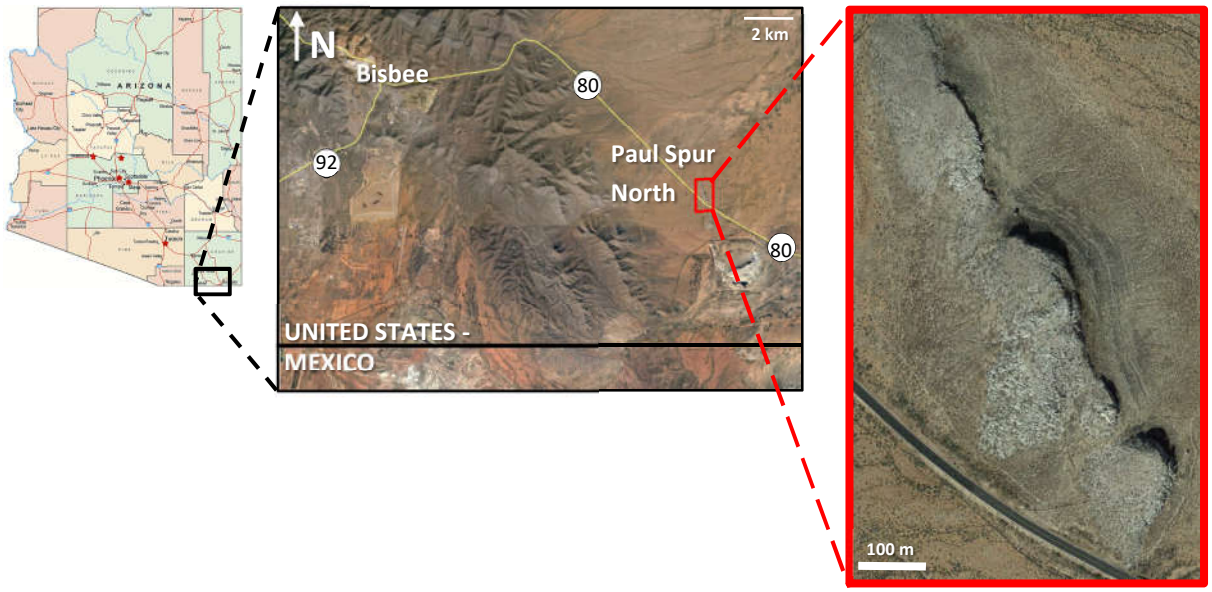

Figure 1: Area map locating study area southeast of Bisbee, Arizona, United States. The outcrop north of Highway 80, boxed in red in the satellite images, is the target of the present study.

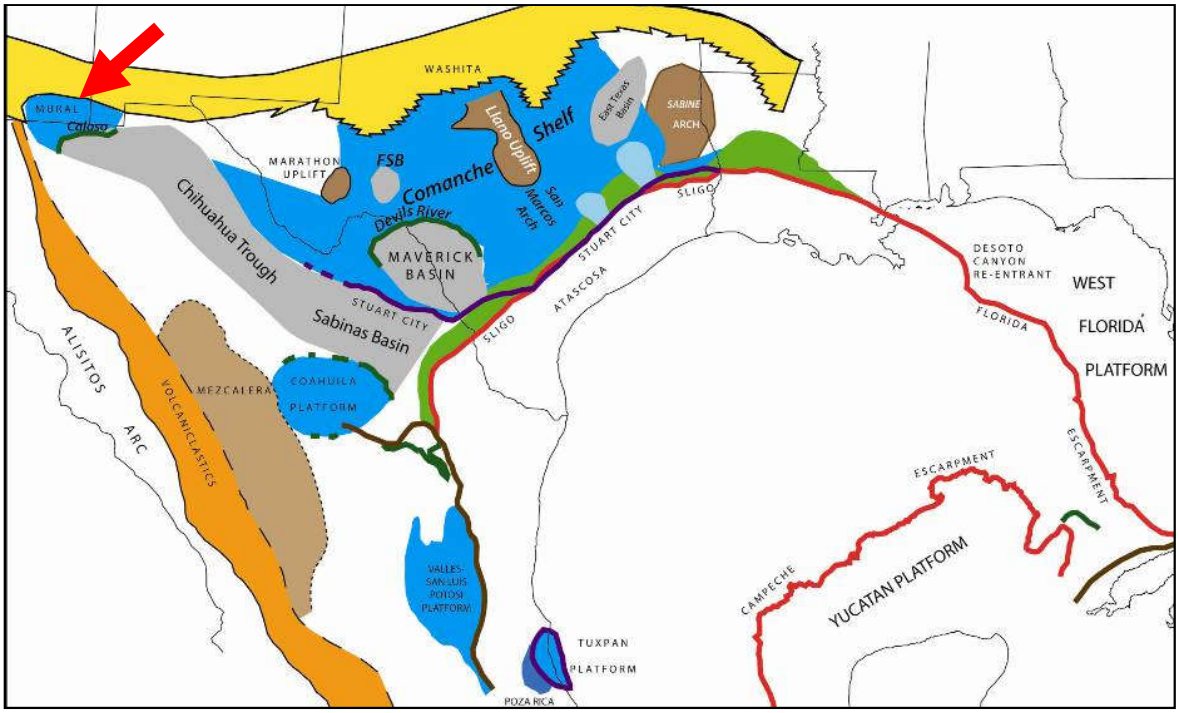

Figure 2: Regional paleogeographic map of Albian southern North America. The Mural Limestone is shown at the northwest end of the Chihuahua Trough. Red arrow shows location of study area. Modified from Kerans (2010).

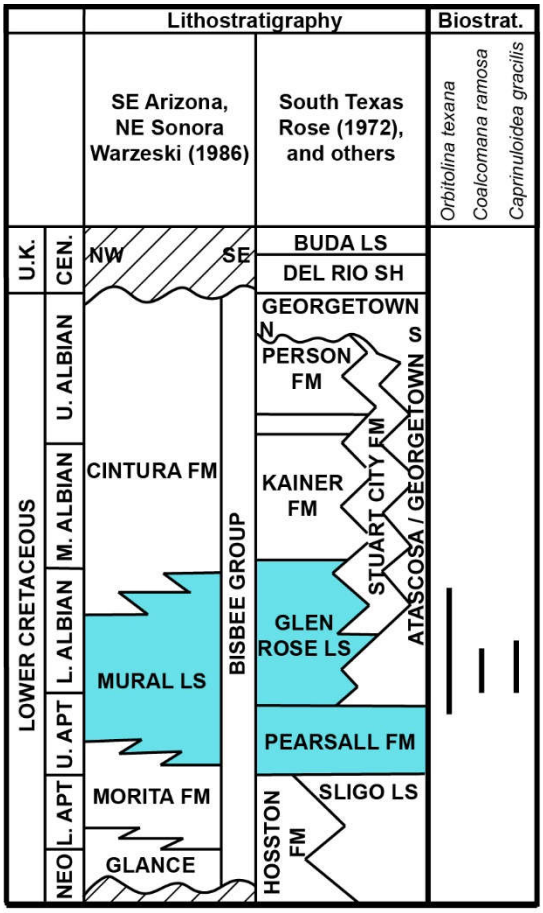

Figure 3: Stratigraphic column of the Bisbee Group, biostratigraphy, and correlative strata in South Texas. Occurrence of *Orbitolina texana* and *Coalcomana ramosa* at Paul Spur places the outcrop in the upper member of the Mural Formation. The Mural Limestone is equivalent to the Pearsall Formation and the overlying Glen Rose Limestone. Modified from Warzeski (1987) and Scott (1987).

Mural is not entirely regressive in nature as previously thought and may instead include a regressive-transgressive-regressive depositional record.

Foraminifer and rudist biostratigraphy places Paul Spur in the latest Aptian to early Albian age (Fig. 3) (Scott, 1987). The large benthic foraminifer, *Orbitolina texana*, is commonly found in late Aptian – early Albian carbonate sediments (Scott, 1987). At Paul Spur, it is abundant in shelfal deposits surrounding and at the base of the reef. The reef biota includes the caprinid *Coalcomana ramosa,* which is restricted to North American uppermost Aptian to Lower Albian reef deposits in the Glen Rose Formation of Texas and the Upper Member of the Mural Limestone of Arizona (Scott, 1981, 1987; Scott and Warzeski, 1993; Scott and Filkhorn, 2007).

CORRELATIVE FORMATIONS

Lithostratigraphic and biostratigraphic work by Hayes (1970), Warzeski (1987), Scott and Filkhorn (2007), Scott and Warzeski (1993), and Gonzalez-Leon et al. (2007) has shown the Mural Limestone to be correlative in age to the Glen Rose Formation and Edwards Group of Texas (Fig. 3). Here, the Glen Rose is of particular interest because it contains patch reefs that may be correlative to patch reefs of the Mural Limestone such as Paul Spur. Two biostratigraphic indicators, the caprinid rudist *Coalcomana ramosa* in reef facies and the benthic foraminiferan *Orbitolina texana* in surrounding open shelf deposits, link the formations closely in age.

Chapter 3: Methods

AERIAL IMAGE ACQUISITION AND PHOTOGRAMMETRIC MODELING

Methods of aerial image acquisition and photogrammetric modeling closely follow those of Zahm et al. (2016). A DJI Phantom III Professional unmanned aerial vehicle (UAV) was used to capture comprehensive aerial images of the outcrop. The UAV includes a self-contained 12 megapixel camera that stores precise GPS spatial data with each photograph. The camera and UAV were remotely monitored and controlled using the DJI Go software on an Apple iPad connected to the controller unit. Images were acquired at distances of approximately 10 meters, 20 meters, and 30 meters from the outcrop with 50% overlap and were taken with a variety of camera angles relative to the rock face to ensure complete coverage. To avoid problems with shadowing and to maintain consistent lighting over the entire outcrop, imaging was only conducted in the morning between the hours of 8:30 and 11:30 AM.

A total of 1,193 images were processed and loaded into Agisoft PhotoScan Professional for development of a three-dimensional model using photogrammetry. Photos were aligned using attached GPS metadata as well as comparisons of like points between images. A high-resolution dense point cloud was generated; point cloud data were then developed into a 3D mesh and texture for export to other applications for manipulation and annotation (Fig. 4A).

HIGH-RESOLUTION FACIES MAPPING

Mapping of facies distributions and geometries on the exposed outcrop top was conducted using a Trimble Pro 6H series differential GPS with decimeter-scale accuracy. Points were taken at intervals between 1 and 3 meters over the entire top surface of the outcrop; additional points were taken in areas of interest such as major facies changes or

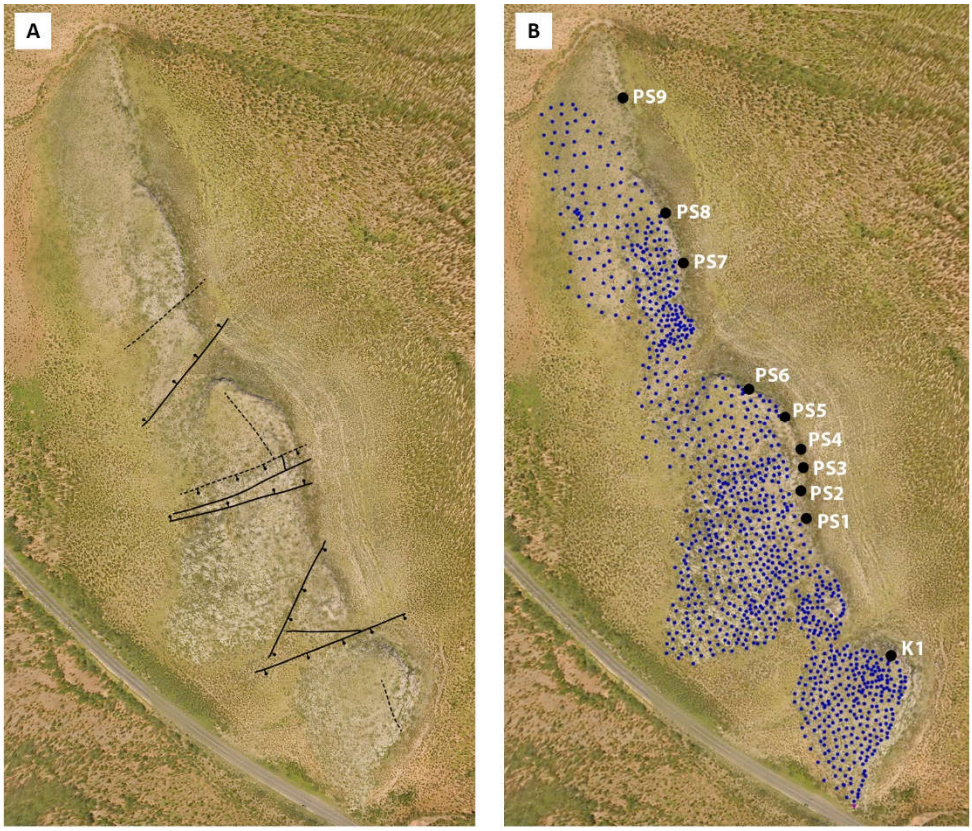

Figure 4: Orthophoto produced from 3D model with overlay of mapped faults **(A)** and stratigraphic column location and differential GPS data points **(B)**. 1,092 points are mapped over the exposed top surface of the reef. Points cluster more densely in areas covered by reefs due to the need to differentiate small-scale changes in reef framework facies. Black dots with labels denote location of measured stratigraphic sections.

contacts. Covered sections were designated by polygons drawn around the perimeter of the areas. A total of 1,092 points were mapped over the exposed platform top; locations of each point are shown in Figure 4B and described in the supplemental data. Each point was associated with a modified Dunham facies classification (Embry and Klovan, 1971) and expanded description of any items of interest. For points including reef material, the ratio of corals to rudists was recorded to aid in analysis of community composition variation. Faults were mapped and offsets were measured where possible (Fig. 4A).

The GPS points were exported from the Trimble Pathfinder software to ArcGIS for development into a high-resolution facies map. The completed map was exported for use as a Google Earth overlay and for use as a base for three-dimensional mapping on the model.

As facies mapping was being conducted, ecological relationships between major reef constituents (i.e. corals and rudists) were recorded. Multiple samples were collected from each facies from a variety of locations on the outcrop; representative samples were cut into thin sections for petrographic analysis, while others were polished as hand samples for analysis of larger-scale structures and relationships.

Further mapping was conducted on the exposed vertical surface on the eastern side of the outcrop using large printouts of photo panoramas shot during a previous field excursion for annotation. Nine stratigraphic sections were also measured and described in detail, as indicated in Figure 4B.

FACIES COMPOSITION ANALYSIS

Seven facies were identified and described based on significant changes in sedimentology, community composition, stratal geometries, and interpreted depositional setting. The composition of each facies was quantitatively assessed to allow better

definition of boundaries, since some reef facies varied substantially. For each facies, 4-7 target sites were selected as representatives for analysis based on quality of preservation, exposure, and clarity of fossil content. Because many corals have a drastically different vertical (cross-sectional) and horizontal (transverse) profile, qualitative compositional estimates were always conducted in the same cross-sectional orientation to avoid error. One site displaying the facies in plan view was also analyzed for each facies for comparison with the cross-sectional view, but was not included in the averaged fossil content analyses.

A meter-squared quadrat was held against each selected site and the area inside the quadrat was photographed with a Canon 5D and a fixed lens. Each quadrat was then reconstructed digitally by stitching together the images in Adobe Photoshop. Foreshortening and skew induced by photographing the quadrat at a slight angle was removed in post processing to restore all visible fossil elements to their correct size.

Two techniques were employed to analyze the composition of the quadrats: point counting and annotation. Point counting was employed for each quadrat following Hamon et al. (2016), with 250 point samples described per quadrat (van der Plas, 1965). Coral elements were subdivided into "platy" (*Microsolena*), "branching/phaceloid", and "massive, miscellaneous, or unidentifiable" categories. Rudist elements were subdivided into "caprinid", "requienid/monopleurid", and "other or unidentifiable" categories. Requienids and monopleurids were counted in the same category because their shell fragments cannot be easily distinguished from one another in outcrop due to a similar two-layered shell structure (Perkins, 1962). Matrix was separated into two categories to reflect the presence of fine, light gray carbonate mud versus coarser, darker grain-dominated packstone. Microbial growth was represented in its own category.

Annotation was utilized primarily to ensure that point counting was obtaining an accurate representation of the facies composition. Each quadrat photo was fully annotated

in a Photoshop overlay with different colors representing different skeletal elements. Because this process was time intensive for some of the more densely populated and complex facies, it was employed for just one representative quadrat per facies.

Chapter 4: Results

The completed three-dimensional model and extensive facies maps clarify vertical succession, reef structure development and architecture, and lateral facies continuity. Paleoecological and facies composition data are used to elucidate the history of reef growth at this locality.

OVERVIEW OF ECOLOGY

Corals and rudists are the major framework components of the Paul Spur patch reef, with corals occupying the dominant reef-builder role through overall higher abundance and larger size. Microbial growth surrounds skeletal elements and forms thick mats on top of platy corals; some encrusting algae have also been identified as *Lithocodium sp.* or *Bacinella sp*. Minor reef constituents, in order of decreasing abundance, include boring bivalves, brachiopods, echinoids, foraminifera, sponges, and bryozoans.

The most commonly occurring coral at Paul Spur is *Microsolena texana*. It presents both massive and thin platy growth forms. The platy morphology is more widespread in outcrop and can either form sheets that grow flat along the substrate or in cup- or V-shaped plates that rise above the substrate. Thick 1-3 cm laminar to stromatolitic microbial mats form on top of the coral plates, and a thin layer of algae (*Lithocodium* or *Bacinella)* encrusts the underside of colonies not directly in contact with the substrate. Mats are not laterally extensive but are instead limited to the top surfaces of *Microsolena.* Lower reef framework is commonly dominated by alternating layers of *Microsolena*, microbial mat, and skeletal packstone matrix forming a nearly monospecific assemblage. *Microsolena* is also common higher up in the reef, though it shares space with other corals and is thus less abundant than in the lower reef.

Other corals observed in outcrop include a variety of growth forms and colony integrations with massive, meandroid, branching, and phaceloid corals all represented. Massive cerioid *Actinastrea* colonies are common throughout the section above the *Microsolena*-dominated facies. Branching and phaceloid corals increase in abundance towards the top of the section; morphology and size are variable, with branches ranging in diameter from 0.5 cm up to 8 cm and coral bodies occupying up to 1 m^3 area, and are not linked to any particular zone of the reef. The largest branching coral colonies can be up to 1 m in diameter in cross-section with branches 6 cm in diameter, whereas the smallest branching or phaceloid corals can have branches less than 1 cm in diameter. Meandroid corals are fairly rare in outcrop, though this may be an artifact of preservation as the intricately coiled surface of the coral is rarely preserved due to erosion, rendering them unidentifiable. Coral diversity increases up-section from one species (*Microsolena)* to over seven species (see Scott, 1981, 1984), though the culminating facies is dominated by rudists.

Rudists are rare in the lower reef (averaging less than 2% abundance) but increase in both diversity and abundance up-section. In lower *Microsolena*-dominated reef facies, the caprinids *Coalcomana* and *Caprinuloidea* are observed reclining on corals or matrix as solitary rare individuals. Stratigraphically higher in the reef, they become common and can occur in locally dense clusters of less than a dozen individuals. The large erect monopleurid rudist *Petalodontia* is common in younger reef strata and is found either living solitarily or in dense clusters supporting one another. Some coiled recumbent requienids (*Toucasia*) may be found in dense muddy thickets up to a meter in diameter. Rare rudists include the diminutive cm-scale elevator monopleurids *Monopleura* cf. *M. marcida*, which are found in small clusters only in the uppermost rudist floatstone facies, and large radiolitids, which occur very infrequently as solitary individuals in upper reef facies. For the most part,

rudists do not preferentially colonize any one zone of the reef; the exception is *Toucasia*, which frequently occurs in association with very fine muddy matrix. Rudists are not observed growing with any spatial preference to corals; cohabitation between corals and solitary rudists is very common in upper parts of the reef framework.

FACIES DESCRIPTIONS

To resolve the depositional history of the patch reef complex, extensive mapping was conducted and nine stratigraphic sections were measured across the outcrop (see Fig. 4). Because the area is faulted (Fig. 4A), the fault offset must be accounted for to provide a clear picture of facies distribution. This was accomplished by "hanging" all of the stratigraphic sections off of the top surface of the skeletal grain-dominated packstone facies, which is laterally continuous and a relatively uniform thickness (3.2-3.5 m) across the outcrop. Facies were then mapped in to create an updated depositional model (Fig. 5).

Seven different facies are described here; for a quick comparison of facies bearing reef-building constituents, see Table 1.

Facies 1: Echinoid-mollusk-Orbitolina mud-dominated packstone

This facies, hereafter referred to as the *Orbitolina* mud-dominated packstone or Facies 1, is most easily identified by its fine texture and the presence of large calcitic benthic foraminifera *Orbitolina texana* (Hofker, 1963), which are visible even to the naked eye in outcrop (Fig. 6A). In outcrop, the *Orbitolina* mud-dominated packstone is light to medium gray in color and occurs in massive beds up to 50 cm thick that weather recessively. Well-preserved *O. texana* up to 4 mm in diameter float in a fine grained skeletal matrix predominantly composed of echinoid and mollusk fragments (Fig. 6B). Other foraminifera, including miliolids, textulariids, and other orbitolinid species, are also present in lower abundances. The top surface of the unit contains extensive large (1-3 cm

		Readily observable components:							
		Microsolena	Microbial growth	Branching coral	Misc. coral	Caprinid	Requienid / Petalodontid	*Monopleura*	Matrix-dominated
Facies	M FRS	x	x						
	DC FRS	x	x	x	x				
	RC BS	x	x	x	x	x	x		
	R RS				x	x	x	x	x
	RD RS					x	x		

Table 1: "Facies at a glance" showing major distinctive features of each reef facies to aid in highlighting differences. M FRS = *Microsolena*-dominated microbial-coral framestone; DC FRS = Diverse microbial-coral framestone; RC BS = Rudist-coral boundstone; R RS = Rudist rudstone; RD RS = Rudist debris rudstone.

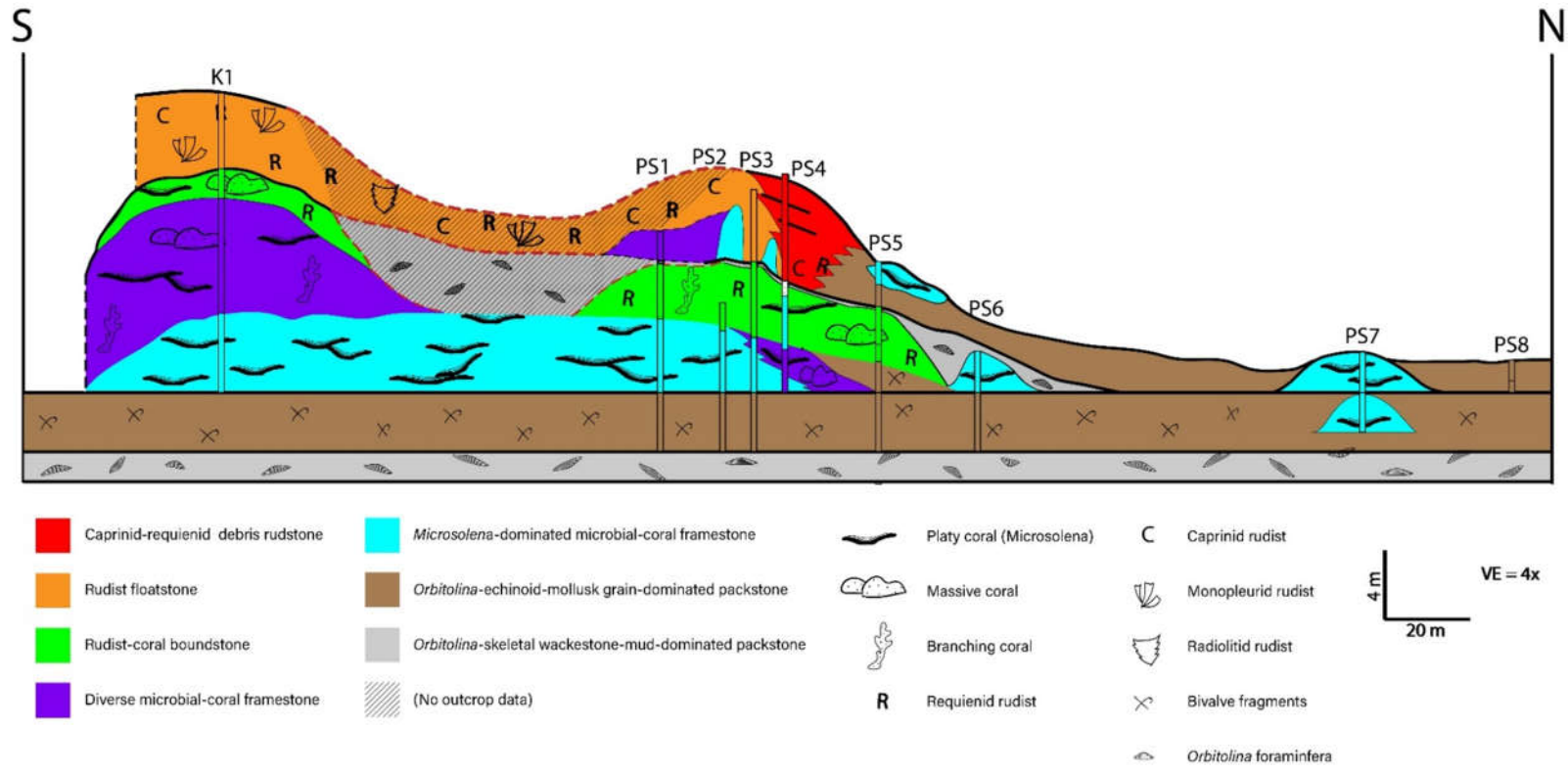

Figure 5: Proposed depositional/stratigraphic model for Paul Spur North. Nine measured stratigraphic sections are shown; model is drawn at 4x vertical exaggeration (VE).

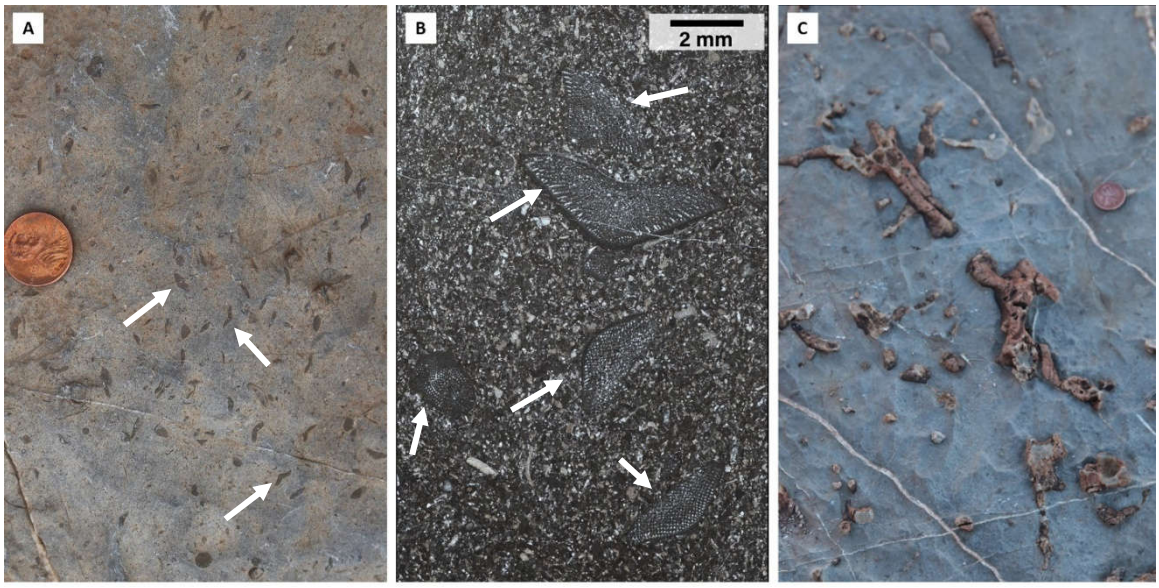

Figure 6: Echinoid-mollusk-*Orbitolina* mud-dominated packstone facies. **(A)** Outcrop view with readily visible *Orbitolina texana* (arrows) floating in a muddy matrix with fine skeletal fragments. **(B)** Photomicrograph of thin section in plane polarized light (PPL). Note variety of sizes of *Orbitolina* (arrows) and poor sorting of skeletal grains. *Sample PS-A1-A-TS (Appendix A).* **(C)** Silicified burrows (brown) preserved in top surface.

diameter) silicified burrows; these burrows also occur throughout the unit in other places, but more sparsely (Fig. 6C).

The *Orbitolina* mud-dominated packstone is visible at the base of the outcrop at Paul Spur North and is gradationally overlain by the *Orbitolina*-echinoid-mollusk grain-dominated packstone. The facies makes a brief reappearance on top of the central reef buildup as a thin (2-30 cm) layer separating two successive reef framework intervals.

Facies 2: *Orbitolina*-echinoid-mollusk grain-dominated packstone

This facies, hereafter referred to as the skeletal grain-dominated packstone or Facies 2, is characterized by coarse, rounded skeletal fragments predominantly composed of echinoid and mollusk fragments (Fig. 7). *Orbitolina* fossils are somewhat rare and abraded in comparison to those found in Facies 1. A thin micritic envelope surrounds most grains. At Paul Spur, the 3-3.5 m thick dark gray to brown unit is massive and laterally continuous across the entire outcrop, where it gradationally overlies the echinoid-mollusk-*Orbitolina* wackestone to mud-dominated packstone and is overlain by reef framework facies.

The skeletal grain-dominated packstone also occurs commonly as beds flanking the reefal facies extending broadly to the north on the leeward side of reef buildups. The skeletal grain-dominated packstone facies is found extensively across the top surface of the northern end of the outcrop and is there referred to as “upper grain-dominated packstone”; in the most northern reaches, this upper unit of grain-dominated packstone likely overlies the lower skeletal grain-dominated packstone unit (see depositional model, Fig. 5). Coral fragments are occasionally present floating in the matrix; the density and size of these large fragments are largely dependent on the distance from an *in situ* reef framework structure. Larger fragments and higher abundances are found closer to the reef framework, and

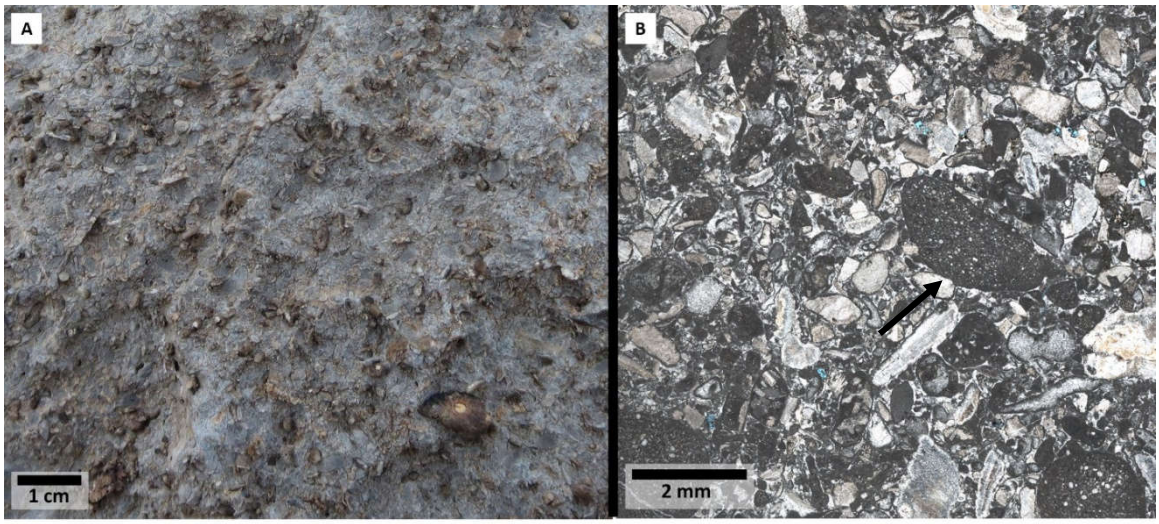

Figure 7: *Orbitolina*-echinoid-mollusk grain-dominated packstone facies. **(A)** Outcrop view of representative sample showing coarseness of grains and abundant molluscan shell debris. **(B)** Photomicrograph of thin section in PPL. Grains are heavily reworked and rounded with poor preservation of fossils such as *Orbitolina* (arrow). Thin micritic envelopes surround most grains. *Sample PS-A2-A-TS (Appendix A).*

skeletal component size and abundance decreases laterally moving away from the reef in flanking beds.

Facies 3: *Microsolena*-dominated microbial-coral framestone

The *Microsolena*-dominated microbial-coral framestone is defined by the dominance of the platy coral *Microsolena* and associated thick (1-3 cm) light gray digitate microbial mats growing on top of the coral plates (Figs. 8, 9A). Muddy to fine skeletal mud-dominated packstone matrix drapes the top of the microbial mats; successive growths of *Microsolena* plates may either rest upon or slightly above the sediment. When the coral grows slightly above the sediment, a thin layer of algae typically encrusts the bottom of the plate.

The average composition of this facies is 34.7% *Microsolena*, 2.6% miscellaneous or unidentified coral, 15.0% microbial growth, 0.4% caprinid rudist, and 46.2% matrix (Fig. 10). This facies is most widespread at the base of the reef directly overlying the *Orbitolina*-echinoid-mollusk grain-dominated packstone, but can also be found in less extensive mounds on the leeward side of larger framestone buildups (see Fig. 5). While the *Microsolena* community at the base of the reef is associated with a very muddy matrix, smaller leeward-side mounds may be associated with a coarser peloid-skeletal matrix. These small reefs are characterized by thinner, more limited growths of *Microsolena* and less extensive microbial buildups.

Facies 4: Diverse microbial-coral framestone

Coral diversity increases up-section with species of branching, massive, and meandroid corals colonizing the reef in addition to *Microsolena* (Figs. 9B, 11). Caprinids are uncommon and solitary. Geopetal structures, when visible, indicate an *in situ* deposition. Void spaces are filled with a skeletal mud-dominated to grain-dominated

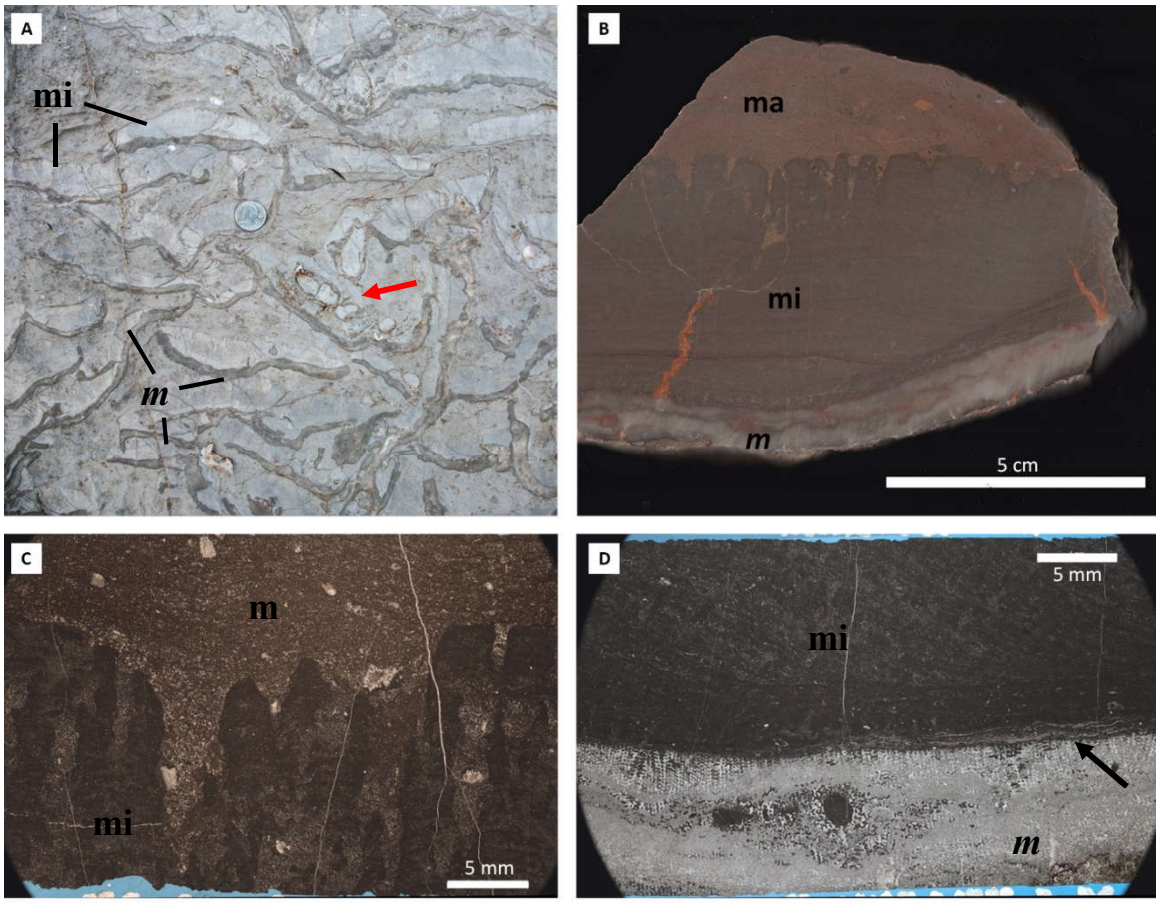

Figure 8: *Microsolena*-dominated microbial-coral framestone facies. **(A)** Cross-sectional view of facies in outcrop. Thin platy *Microsolena* (*m*) support thick digitate microbial mats (mi). Medium-coarse skeletal mud-dominated matrix filling around coral and mats. Rare caprinid (*Coalcomana*) present (red arrow). **(B)** Polished hand sample showing relationship between *Microsolena* (m), microbial mat (mi), and matrix (ma). *Sample PS-A9 (Appendix A).* **(C)** Photomicrograph (PPL) of interface between top of microbial mats and overlying matrix; note digitate morphology of top of microbial mats (mi). *Sample PS-A9-A-TS (Appendix A).* **(D)** Photomicrograph (PPL) of interface between *Microsolena* (*m*) and microbial mat (mi). Note encrusting algae directly on top of coral between coral and mat (arrow). PPL. *Sample PS-A9-C-TS (Appendix A).*

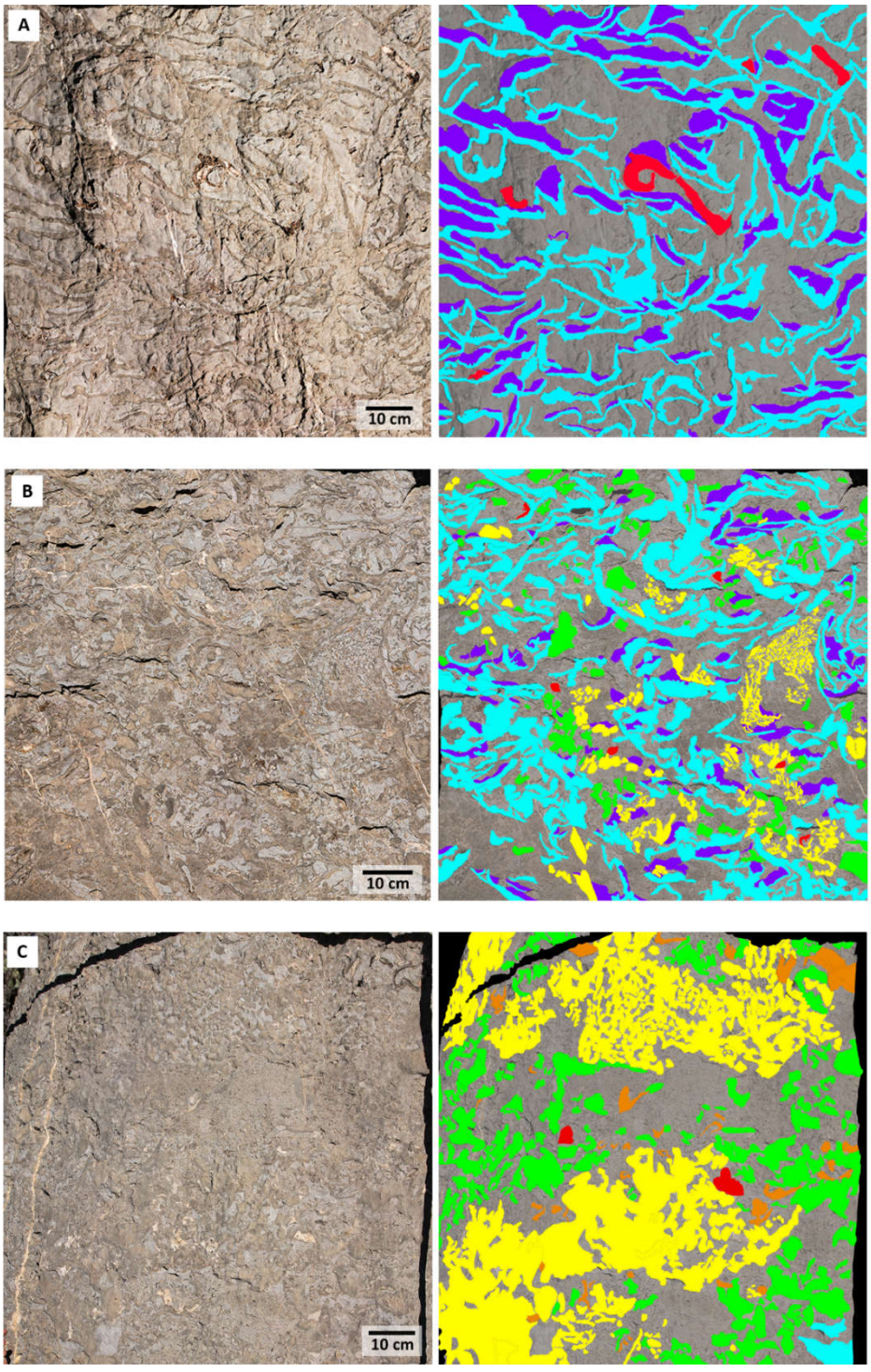
A
10 cm
B
10 cm
C
10 cm

Figure 9 (previous page): Representative quadrats displaying typical composition and texture of reef facies. Original photo on left and annotated photo showing fabrics on right. Blue = *Microsolena*; purple = microbial growth; red = caprinid rudist; yellow = branching corals; green = miscellaneous or unidentifiable corals; orange = requienid or petalodontid rudist. **(A)** Q1: *Microsolena*-dominated microbial-coral framestone facies containing 28.7% *Microsolena,* 15.9% microbial growth, and 53.8% very fine muddy packstone matrix. Caprinids rare at 1.6% abundance. 53.8% of the quadrat is composed of a very fine muddy packstone matrix. **(B)** Q19: Diverse microbial-coral framestone facies containing 29.4% *Microsolena*, 6.4% branching coral, 5.8% massive or unidentified corals, 5.9% microbial growth, and 52.2% mixed carbonate mud and coarse grain-dominated packstone. **(C)** Q28: Rudist-coral boundstone facies containing 33.9% branching corals, 17.8% massive or unidentified corals, 3.2% rudists (caprinids, petalodontids, and requienids), and 44.9% mixed carbonate mud and coarse grain-dominated packstone matrix.

Figure 10 (next page): Facies compositions for each sampled quadrat. Quadrats are grouped by facies type; each group is headed by the averaged facies composition. Note the significant variation in the rudist-coral boundstone facies compared to all other reef facies.

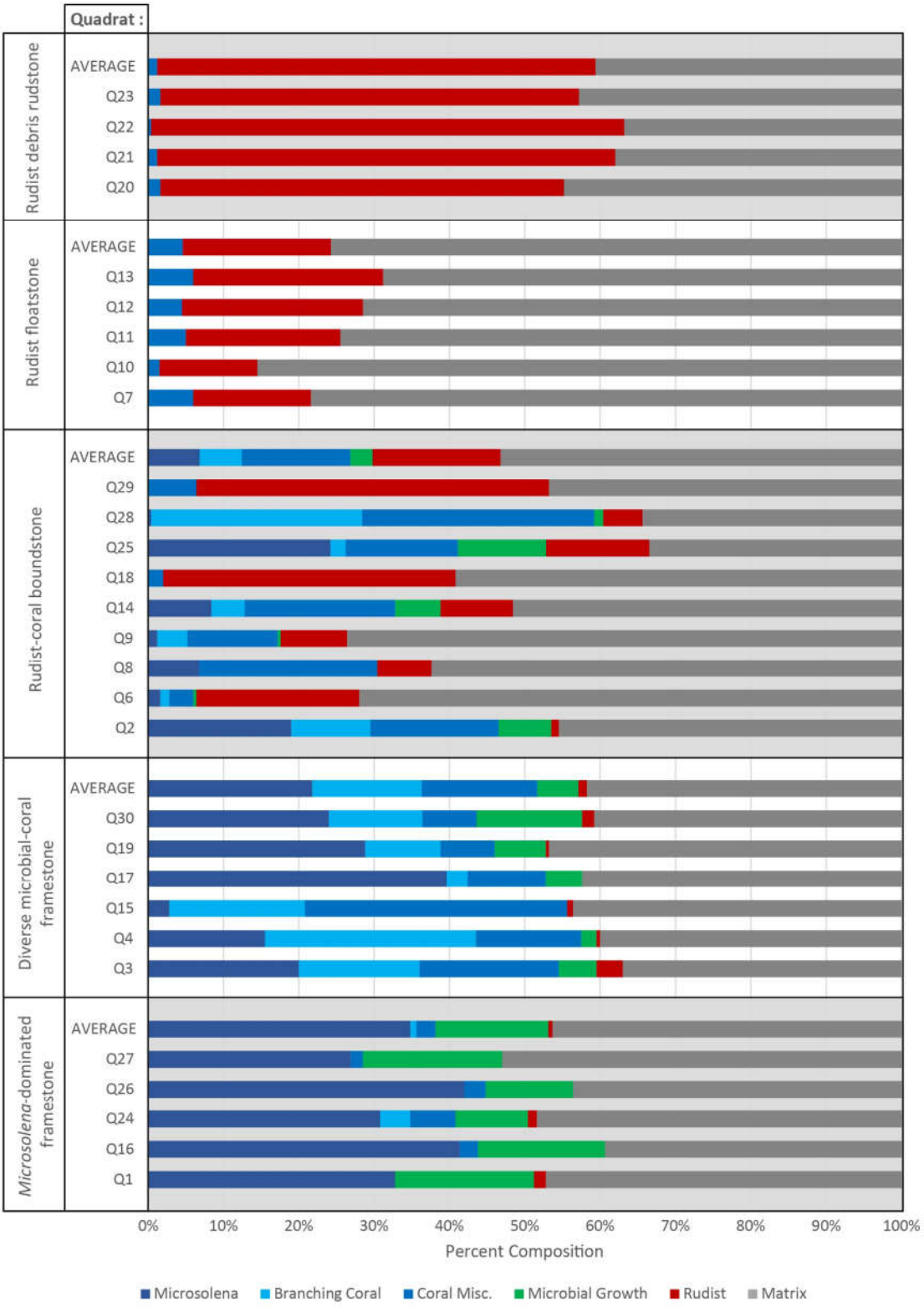
Quadrat :
Rudist debris rudstone
AVERAGE
Q23
Q22
Q21
Q20
Rudist floatstone
AVERAGE
Q13
Q12
Q11
Q10
Q7
Rudist-coral boundstone
AVERAGE
Q29
Q28
Q25
Q18
Q14
Q9
Q8
Q6
Q2
Diverse microbial-coral framestone
AVERAGE
Q30
Q19
Q17
Q15
Q4
Q3
Microsolena-dominated framestone
AVERAGE
Q27
Q26
Q24
Q16
Q1
0%
10%
20%
30%
40%
50%
60%
70%
80%
90%
100%
Percent Composition
Microsolena
Branching Coral
Coral Misc.
Microbial Growth
Rudist
Matrix

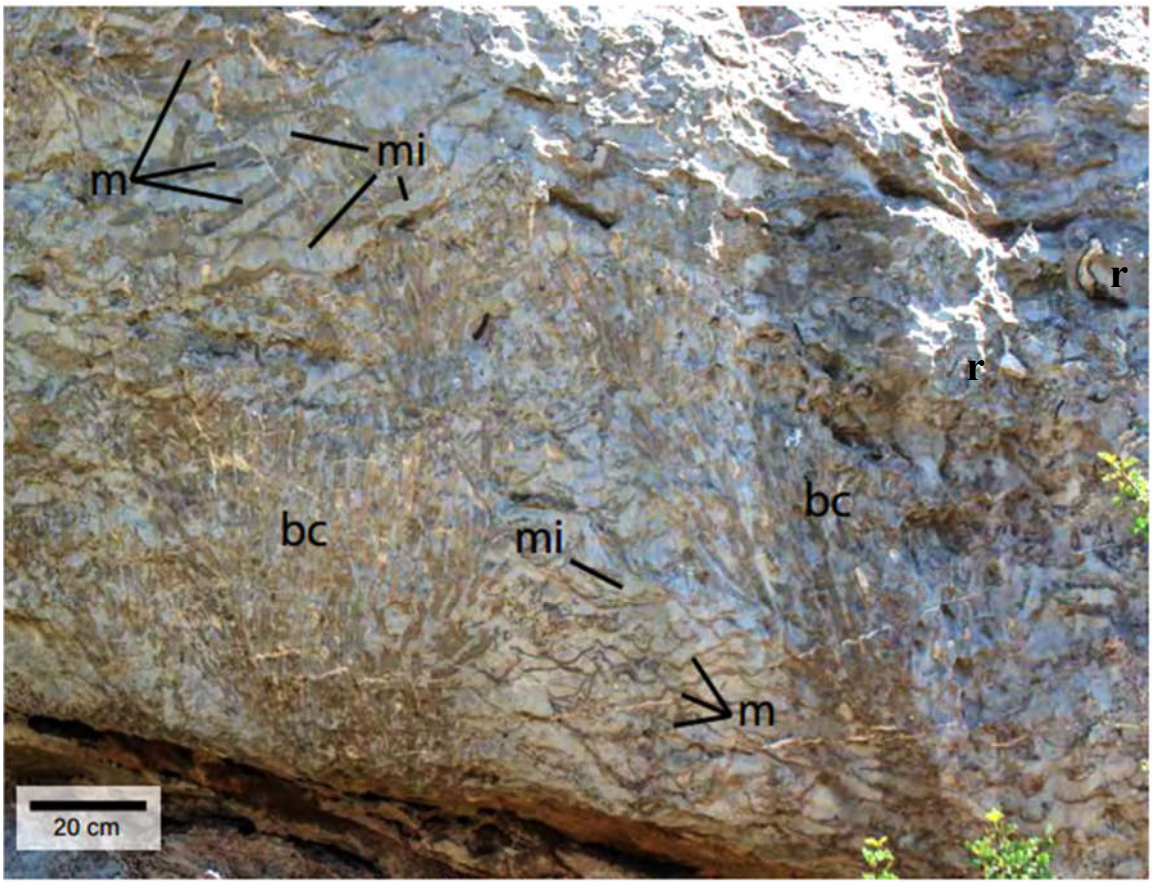

Figure 11: Diverse microbial-coral framestone facies. Coral diversity is high with branching corals (bc) and small massive corals present in addition to the *Microsolena* and microbial mats (m and mi, respectively) seen lower in section. Few caprinids (r) visible.

packstone matrix containing varying amounts of poorly sorted mollusk, echinoid, coral, and rudist fragments. Muddier variations of this facies are easily recognized by their light gray matrix color in outcrop, while more grain-dominated facies take on a brown-gray hue. The average composition of this facies is 51.7% coral, 21.8% of which is *Microsolena*, 14.5% branching coral, and 15.4% miscellaneous or unidentifiable coral (Fig. 10). Microbial mats are not as extensive as in the *Microsolena*-dominated framestone, with a 5.4% abundance. Caprinid rudists remain rare at an average of 1.1% of reef composition and matrix fills 41.8% of the framework.

Buildups of this facies typically succeed the *Microsolena*-dominated coral framestone. While the *Microsolena*-dominated facies is more laterally than vertically extensive, accumulating a maximum of 4.6 m of vertical growth and extending for 440 m north-south in outcrop, the diverse coral framestone facies builds more vertical topography with less lateral accumulation. On the southern end of the outcrop, this facies builds significant topography with a maximum vertical growth of 6.2 m and a lateral extent of 140 m.

Facies 5: Rudist-coral boundstone

The rudist-coral boundstone is similar in texture to the diverse microbial-coral framestone but is differentiated by the presence of petalodontid and requienid rudists (Figs. 9C, 12). It is the most diverse of all facies described here as the ratio of corals to rudists can vary by as much as 47% (Fig. 10). In one sampled area, corals comprise 46.5% of the measured quadrat (Q2) and rudists are only 1.0%; in another sample (Q6), only 6.0% is composed of corals in comparison to 21.6% rudists. Spatial variability is high even in samples only a meter apart. Averaging nine sampled sections yields a value of 26.8% coral and 17.0% rudist composition.

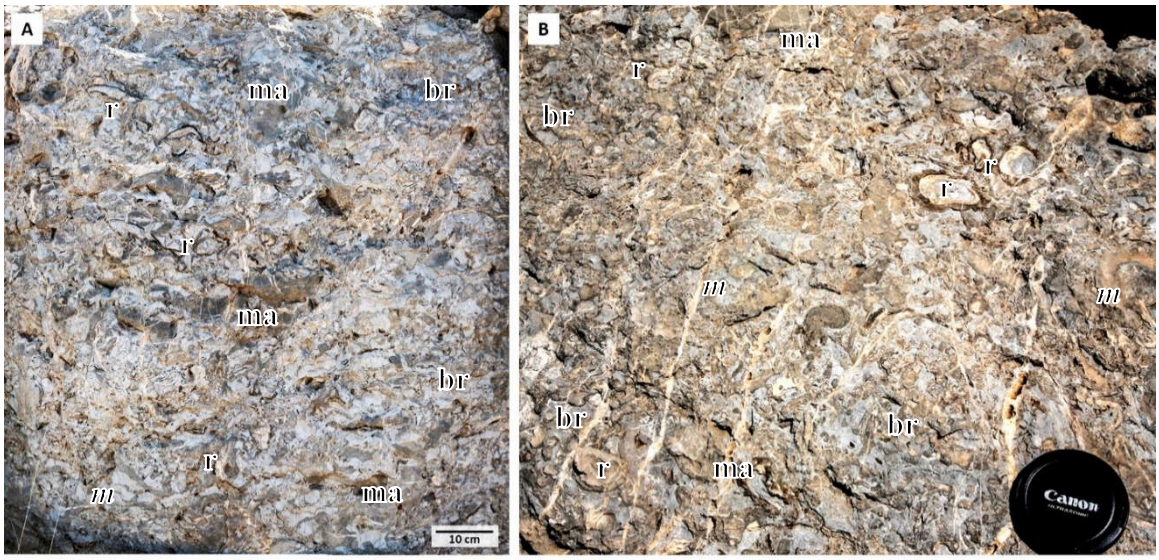

Figure 12: Rudist-coral boundstone facies. Requienid and petalodontid rudists (r) are mixed in with a diverse assemblage of corals (br = branching, ma = massive, *m* = *Microsolena*). Rudists typically occur as solitary individuals, though limited colonial clusters may occur in some parts of the facies. **(A)** Representative view of facies in cross-section. **(B)** Plan view of the facies. Note that this facies may vary substantially in appearance and faunal composition when viewed at a meter-scale resolution as seen here; see Figure 10.

Rudists occur as solitary individuals living intermixed with corals, or may appear in small bouquet-like clusters with a few other individuals. Uncommonly, they form localized dense meter-scale assemblages within a grain-rich matrix. Caprinids remain uncommon in comparison to requienids and petalodontids, making up a maximum of 10.0% of the fabric but averaging 3.4% abundance (Fig. 10).

Microbial mats are infrequent in comparison to Facies 3 (average 3.0% in sampled sections), and growth more typically occurs in the form of extensive algal (*Lithocodium sp.* or *Bacinella sp.*) encrustations on other organisms. The matrix of this facies is predominantly grain-rich packstone that comprises an average of 53.2% of sampled reef fabrics.

The rudist-coral boundstone is found higher up in the reef section, typically overlying either the diverse microbial-coral framestone or the *Microsolena*-dominated microbial-coral framestone. On the southern end of the complex, it forms a relatively thin (1.7 m) cap covering the 6.2 m thick diverse microbial-coral framestone growth. To the north, it occurs in a thicker package up to 4.4 m thick overlying the *Microsolena*-dominated microbial-coral framestone and the diverse microbial-coral framestone.

Facies 6: Rudist floatstone

The rudist floatstone is largely matrix-dominated (average 75.7% of total composition of each sample) and contains significantly less coral than previously described facies (average 4.6%; Fig. 10). Corals are fragmented and appear to be predominantly rubble rather than *in situ* growths. The major reef constituents of this facies are *in situ*, toppled, or fragmented rudists (19.7%; Figs. 13, 14A).

Rudist diversity in this facies is the highest seen in this outcrop with requienids, caprinids, radiolitids, and monopleurids (both *Petalodontia* and *Monopleura)* all present.

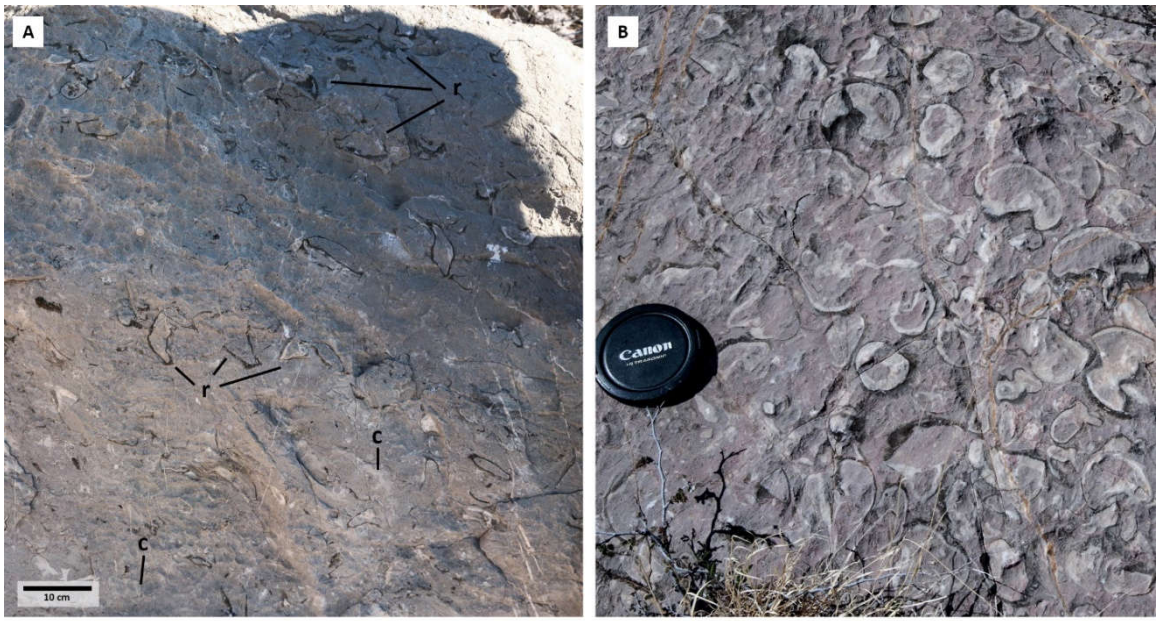

Figure 13: Rudist floatstone facies. Rudists (r) typically float *in situ* in a coarse, grain-rich matrix with uncommon coral fragments (c) **(A)**; however, some parts of the facies may contain limited dense colonies of requienids in a somewhat muddier packstone matrix **(B)**. These "thickets" of rudists are no more than 2 m in diameter.

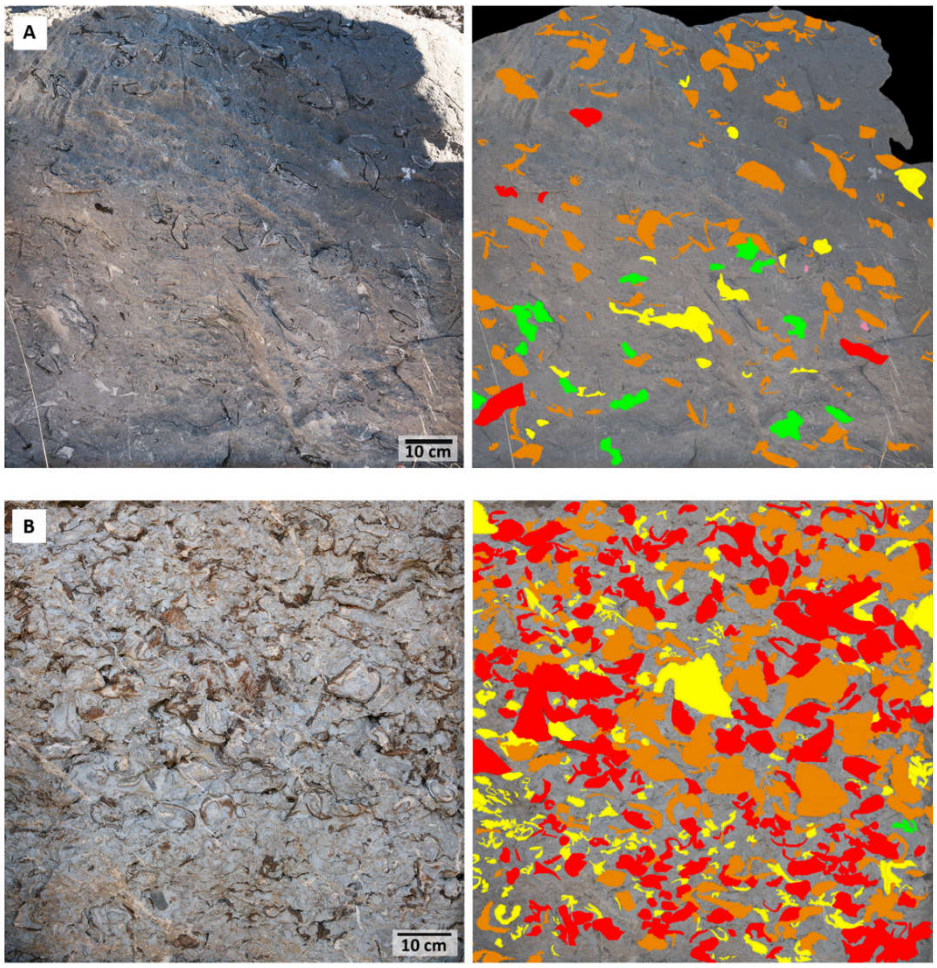

Figure 14: Representative quadrats displaying typical composition and texture of reef facies. Original photo on left and annotated photo showing fabrics on right. Red = caprinid rudist; yellow = miscellaneous or unidentifiable rudists; green = miscellaneous or unidentifiable corals; orange = requienid or petalodontid rudist; pink = *Monopleura*. **(A)** Q11: Rudist floatstone facies composed of coarse grain-dominated packstone matrix (85.8%), requienids and petalodontids (9.4%), caprinids (1.1%), miscellaneous or unidentified rudists (1.7%), and coral fragments (2.0%). **(B)** Q22: Rudist debris rudstone facies containing 24.4% caprinids, 20.5% requienids and petalodontids, 8.8% miscellaneous or unidentifiable rudists, and 46.5% mixed carbonate mud and grain-dominated packstone matrix.

Requienids and petalodontids remain the most common rudist type (13.4%) and occur most commonly as solitary individuals or in small closely-packed clusters (Fig. 13A). Uncommonly, they may be found in dense clusters or thickets surrounded by a light gray medium to fine skeletal lime mud matrix (Fig. 13B). Caprinids are mostly solitary but may be found grouped in loose clusters of less than ten individuals. Large radiolitids are also mostly solitary. In contrast, small (<6 cm tall) conical elevator *Monopleura* are found exclusively in tightly packed bouquet-like clusters. The abundance of this monopleurid varies within the facies but is difficult to establish because of this clustering behavior. Additionally, it should be noted that *Monopleura* is only found near the top of the facies on the southern side of the complex, which is covered in vegetation that hinders facies sampling. Thus, overall monopleurid abundance in the facies is higher than represented by sampling efforts.

Facies 7: Rudist debris rudstone

This distinctive facies is characterized by an abundance of mixed large petalodontids, caprinids, and requienids densely packed in a fine muddy packstone matrix (Figs. 14B, 15). Most rudists are intact but not in place, suggesting that they were transported a short distance before deposition. In the top 50 cm of the unit, the rudists are highly fragmented (Fig. 15B). Rudists make up an average of 58.2% of the facies composition (27.4% caprinid, 23.3% requienid / monopleurid, and 7.5% other or unidentifiable rudist) with matrix comprising the rest (40.6%; Fig. 10).

This facies is occurs only in the uppermost reef on top of one buildup (Fig. 5). It is deposited in meter-scale inclined flanking beds dipping approximately 12 degrees to the north on the leeward side of the reef and grades out into the skeletal grain-dominated packstone to the north.

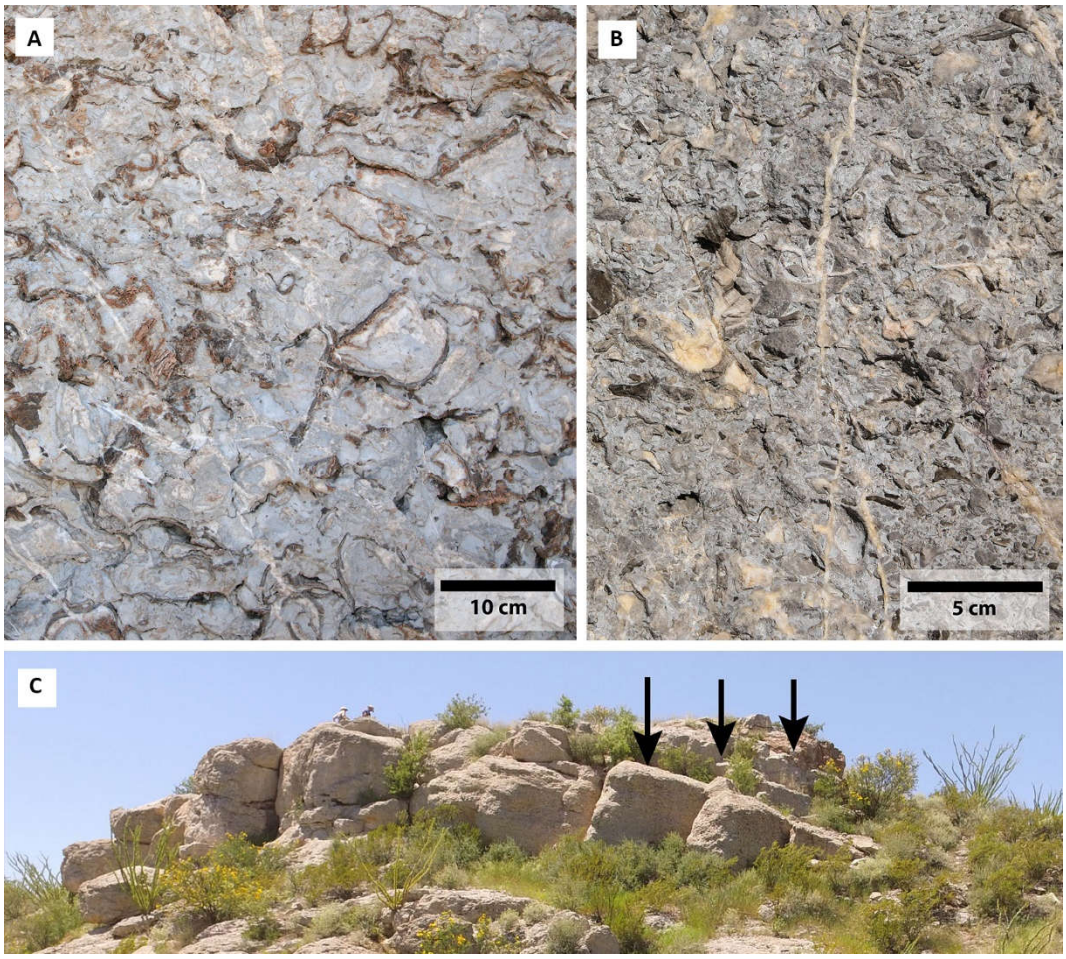

Figure 15: Rudist debris rudstone facies. Massive poorly-sorted facies composed primarily of very large intact **(A)** to medium fragmented **(B)** petalodontid, caprinid, and requienid rudist skeletal fragments in a mixture of carbonate mud and grain-dominated packstone matrix. **(C)** Inclined meter-scale bedding dipping to the north (indicated by arrows) is evident in outcrop.

DIRECT CORAL-RUDIST ECOLOGICAL RELATIONSHIPS

Though reliable instances of definite overgrowth are somewhat rare, rudists and corals are observed directly interacting with one another in several instances in outcrop (Figs. 16, 17). Direct interactions are defined by definite observable overprinting or growth relationships. Simple close stratigraphic association is not considered to be a direct interaction; neither is association of elements not preserved *in situ*. As such, only a dozen examples of direct interaction have been documented in outcrop.

Platy or massive corals more frequently grow over rudist clusters than rudists growing on top of corals (10 out of 12 documented interactions). Corals observed overgrowing rudists included *Actinastrea* and *Microsolena*; these were large corals that grew indiscriminately over clusters of rudists rather than growing upon and encrusting individual rudists (Fig. 16, A-B and E-F). However, in one instance a massive meandroid coral was observed either growing on or up against a singular rudist (Fig. 16, C-D). Rudists that were overgrown were recumbent caprinids and requienids.

Occurrences of rudists growing on corals were rare, but when observed occurred as growths on branching corals (Fig. 17). It is impossible to know if these rudists colonized the coral prior to or after its death, because branching corals often remain intact and upright for some time after death if not disturbed. No rudists were observed colonizing the top surfaces of platy or massive corals.

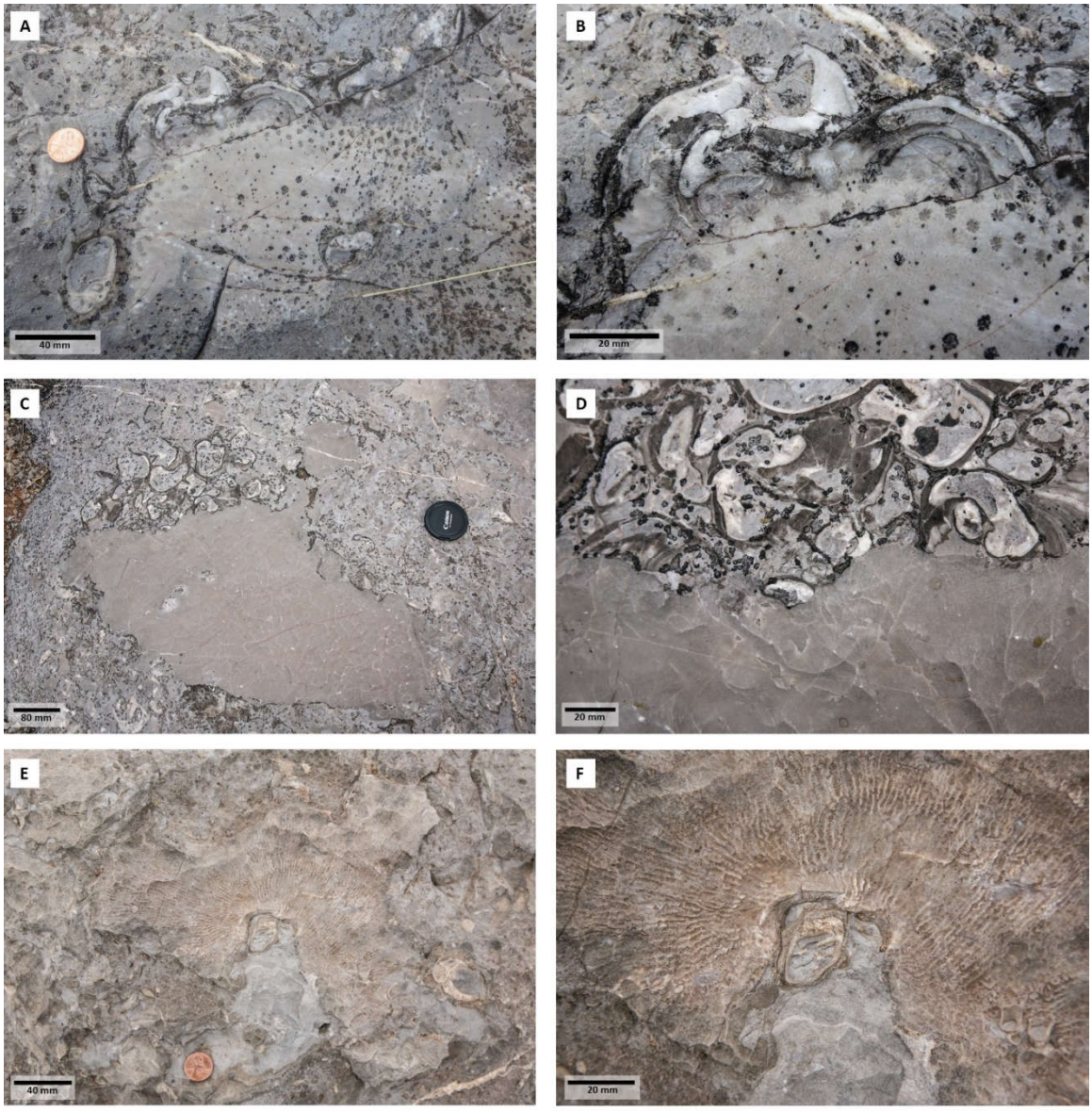

Figure 16: Examples of direct coral-rudist interactions in the form of overgrowth relationships. **(A)** Top-down view of *Actinastrea* overgrowing several caprinids. **(B)** Close-up view of overgrowth shown in (A). **(C)** Top-down view of platy coral *Microsolena* overgrowing thicket of requienids; **(D)** shows close-up view of overgrowth relationship. **(E)** Top-down view of meandroid coral growing either on or around a rudist; **(F)** is expansion of center of (E) showing close-up view of coral butting up to rudist; rim of coral associated with algal growth and rudist shell surrounded by marine cement.

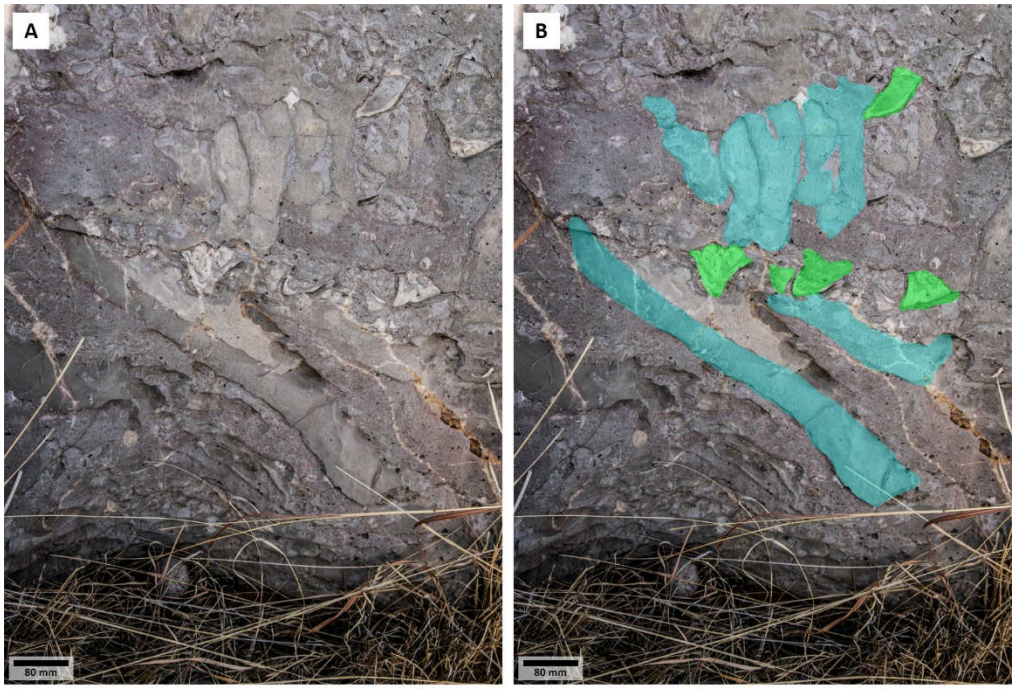

Figure 17: Example of rudists (likely petalodontids) growing on a large branching coral. An unidentified massive coral (arrow) is also supported in the branches and may be the substrate upon which one of the rudists is growing. Note the upright orientation of the rudists that is indicative of *in situ* preservation. **(A)** Original image; **(B)** Annotated with blue highlighting the body of the branching coral and green highlighting the upright rudists.

Chapter 5: Interpreted Depositional History

This study presents a new look at the biotic communities of Paul Spur and their relationship with reef development through time. Though some facies such as the *Microsolena*-dominated microbial-coral framestone remain the same by definition (compare to Aisner, 2010; Roybal, 1981; Scott, 1979, 1981; Scott and Brenckle, 1977), their interpretation is significantly different in some cases. This, in turn, prompts new insight into environmental factors impacting growth of the reef complex, as well as mechanisms mediating the interplay of coral and rudist communities.

The *Orbitolina* mud-dominated packstone, which is the basal unit at Paul Spur predating development of the reef (Fig. 18A), has been widely interpreted as an open marine facies (e.g. Scott, 1979; Aconcha, 2008; Aisner, 2010). The defining disc-like *Orbitolina* foraminifera and fine peloid-skeletal matrix are both characteristic of a subtidal quiet marine setting. The unit's massive habit is likely a result of bioturbation; additionally, common large silicified burrows indicate that it was deposited during a time when waters were well-oxygenated and biota were unstressed.

The thick (3.2-3.6 m) skeletal grain-dominated packstone that followed deposition of the *Orbitolina* mud-dominated packstone is composed predominantly of coarse molluscan skeletal material sourced from allochthonous reef debris and shelf material reworked by wave action, currents, and storm activity (Fig. 18B). Common *Orbitolina* fossils are poorly preserved and abraded, but are notably taller in morphology than the *Orbitolina* found in the *Orbitolina* mud-dominated packstone, indicating a shallower water depth (Vilas et al., 1995; Pittet et al., 2002; Schroeder et al., 2010). Small *Microsolena*-dominated microbial-coral framestone buildups may have developed during this phase, but did not establish significant topography in comparison to the main reef buildup that was

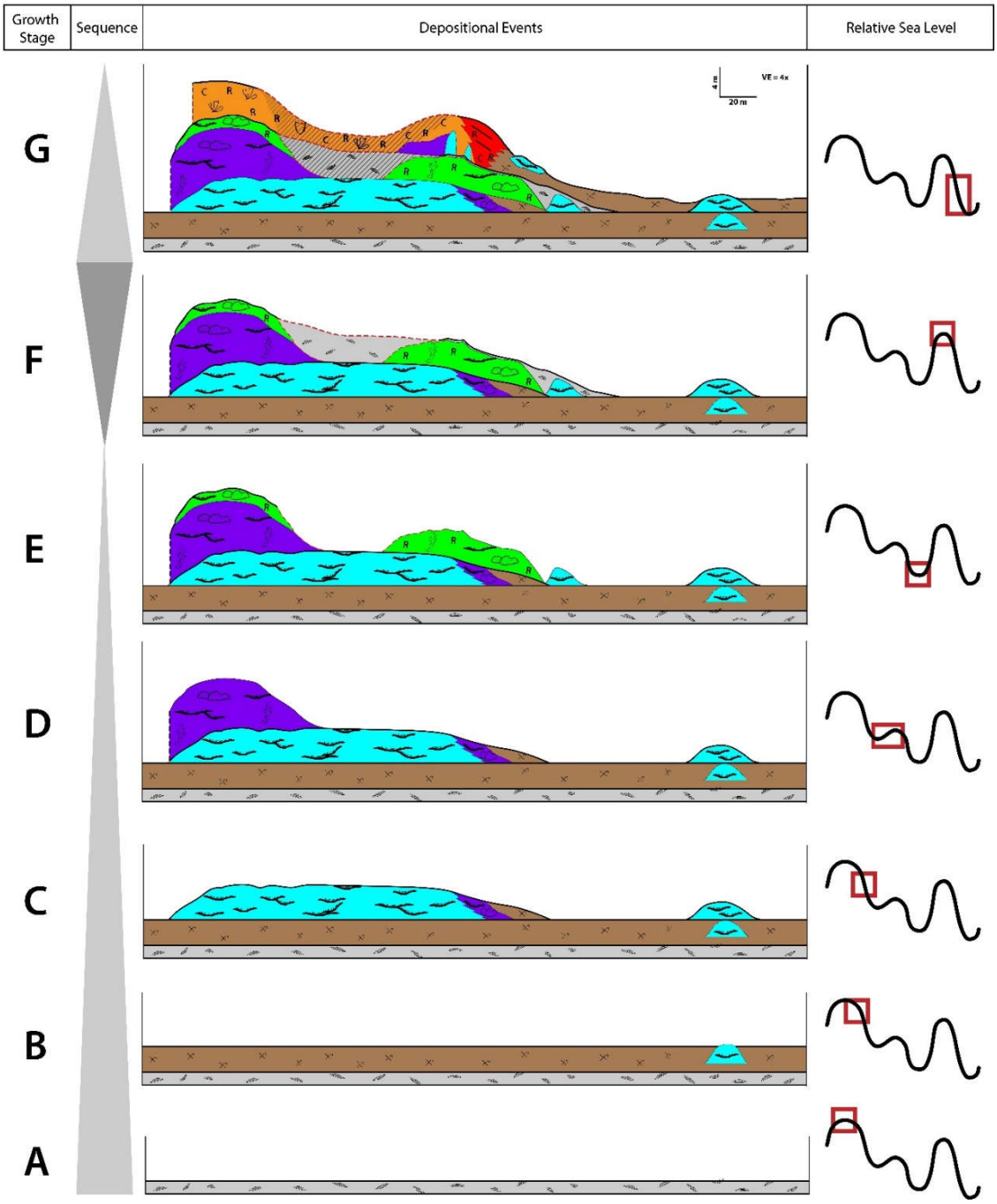

Figure 18: Deconstructed depositional model illustrating stages of reef development and correlation to local relative sea level fluctuations as a potential mechanism controlling reef architecture and community distribution. Note: vertical exaggeration is 4x. Facies and symbols as in Figure 5.

established later, growing to less than 1.5 m in height and less than 2 m diameter at the base of the buildup.

The skeletal grain-dominated packstone facies has been previously interpreted as a back reef shoal (Scott, 1979; Aisner, 2010) due to its coarse skeletal, fragmental composition. This interpretation is still supported though it should be noted that the thickness of the unit (3.2 to 3.5 m) may be unusual for a back reef shoal unless significant degradation of the reef was taking place. Absent bedforms point to mobile sediments and high sedimentation rates; therefore, the primary mechanism driving the development of this unit was strong wave energy and currents. The inferred shallower water depth may help explain the development of this unit: if a reef with significant vertical growth developed basinward in deeper water during a period of higher sea level, a regression would cause it to come into contact with wave base. Increased wave action would have contributed to significant erosion as sea level dropped during the shoaling upwards cycle, providing the coarse sediments that sourced the skeletal grain-dominated packstone.

Occurrences of the grain-dominated packstone can be observed elsewhere in outcrop, typically in small meter-scale gaps in the reef framework and in small debris "tails" extending off of the north side of buildups. These debris facies have previously been used to determine paleocurrent direction, as they are interpreted to be back reef shoals generated by breakdown and transport of reef structures by wave action and currents. Our data here are in agreement with previous assessments (e.g. Aisner, 2010; Roybal, 1981; Scott and Brenckle, 1977): paleocurrents ran north-northwest from the south-southeast.

Eventually, the thick skeletal grain-dominated packstone shoal acted as the initiation point for the first stage of reef growth, which was predominantly *Microsolena*-dominated microbial-coral framestone (Fig. 18C). The *Microsolena*-dominated microbial-coral framestone is an unusually low-diversity reef facies found consistently in Aptian and

Albian Gulf Coast reef assemblages in a variety of different settings. It is extensively documented throughout the patch reefs of the Mural Limestone of the Bisbee Basin (Monreal, 1985; Roybal, 1981; Scott, 1979, 1981, 1990; Scott and Brenckle, 1977) and the James Limestone of Texas (Achauer and Johnson, 1969; Greenberg, 1986). It is observed in the Running Duke Field (Rodessa Formation) in what has been interpreted as a reef belt landward of the shelf margin reef, though depositional models are not in agreement as far as mechanisms of reef growth (Scott, 1990). Futhermore, the facies is also found in the Stuart City reef margin in the lower reef framework (Bebout and Loucks, 1974; Scott, 1990). Despite the nearly-identical composition and growth habit reported by all of these studies, different workers have attributed this facies to disparate reef zones and times of growth. In the Mural Limestone, this facies has previously been attributed to the "middle reef", or a growth stage of the reef occurring after initial establishment of pioneering massive corals (Scott and Brenckle, 1977; Scott, 1979,1981). It has also been interpreted as a reef crest facies dominated by intense wave energy (Roybal, 1981). In the James Limestone, the *Microsolena*-microbial mat association is reported as being indicative of a somewhat deeper water subtidal environment (Achauer and Johnson, 1969; Greenberg, 1986). In the Rodessa Formation, it is once again attributed to a second-generational middle reef community (Scott, 1990), though it should be noted that the depositional model is taken from Scott and Brenckle's (1977) model of the Mural patch reefs. Finally, in the Stuart City reef, the *Microsolena*-microbial faces is depicted as a deeper water facies at the base of the reef frame overlying the forereef slope (Bebout and Loucks, 1974; Scott, 1990, 1995). Reports of water depth for this shelf margin community vary from very shallow (10-30 feet) (Bebout and Loucks, 1974) to deeper than 10 meters (Scott, 1995).

With the revision of the history of reef growth and stratigraphy at Paul Spur, the *Microsolena*-microbial facies in the Mural Limestone falls in line with the interpretations

made for the James Limestone patch reefs and for the Stuart City shelf margin reefs. Rather than being a secondary generation of reef growth mediated by wave action and currents, as originally proposed by Scott and Brenckle (1977), the *Microsolena*-microbial framestone is instead a pioneer reef facies, initiating growth of the reef upon a skeletal grain-dominated packstone shoal. The thick microbial mats and fine lime mud matrix associated with *Microsolena* supports growth in a quiet, deeper-water marine environment where wave action was unlikely to disturb the accumulation of mud. This interpretation is also more consistent with what is known about modern platy coral growth morphologies, which are typically found in deeper water environments where corals are somewhat stressed and must maximize surface area to acquire enough light (Fricke and Schuhmacher, 1983; Rosen et al., 2002). The reef framework built by these corals grew outwards (laterally) more than upwards (vertically), which is typical of low-relief platy coral growth. Lateral growth could also represent limited accommodation space due to shallow water, but is unlikely here given the apparent muddiness of the environment and lack of wave energy.

After the first stage of reef growth, coral alpha diversity increased drastically with the addition of over a dozen species of branching, phaceloid, meandroid, and massive corals (see Scott, 1981); this high diversity defines the diverse microbial-coral framestone community (Fig. 18D). While *Microsolena* maintained a strong presence (averaging 42.2% of reef builders), the platy corals were no longer as extensive and laterally continuous as in the previous stage of growth. The fine carbonate mud matrix observed in the microbial-*Microsolena* facies is less prominent and appears mixed with a coarser skeletal grain-dominated packstone matrix or as small pockets in the shelter of corals. The overall nature of the reef growth is altered as well, with greater vertical accumulation than recorded in the *Microsolena* facies and comparatively less lateral accumulation. Its taller, narrower shape was not likely entirely mediated by the taller growth forms of the larger massive and

branching corals. Instead, I propose that the reef during this time may have been employing a "keep-up" strategy (Neumann, 1985), growing upwards into accommodation space to stay in the optimal water depth as local sea level rose slowly. Alternatively, it could have successfully established itself on top of the *Microsolena*-dominated reef buildup during an initial minor shallowing, and then simply grown up to fill all available accommodation space as sea level remained constant.

During the initial period of diversified coral reef growth, rudists were very rare and were usually solitary recumbent caprinids that reclined in the substrate in the shelter of the larger corals. As time progressed, requienid and petalodontid rudists colonized the reef community as well, defining the rudist-coral boundstone facies (Fig. 18E). This facies forms a thin (1.7 m maximum thickness) cap covering the diverse coral framestone buildup as well as a larger reef buildup to the north. Reef growth is more lateral than vertical, similar in shape to that of the *Microsolena*-dominated facies; however, here the lateral growth is more suggestive of a limitation in accommodation space possibly caused by shallowing. Large massive and branching corals typical of shallow water reefs continue to dominate alongside the requienids and petalodontids, which are also known for their preference for shallower environments (Perkins, 1962, 1974). The fine carbonate mud matrix seen in deeper facies is almost entirely absent here, having been replaced by the coarse skeletal grain-dominated packstone matrix more typical of a higher-energy environment.

Because the rudist-coral boundstone facies is so similar to the diverse coral framestone facies, having only one major different fossil constituent (i.e. the presence of rudists), it is likely that the two associated reef growth phases were built within a short time of one another. Continued upwards shallowing likely limited development on the top of the taller reef structure but did not inhibit the establishment of a new buildup in the back

reef area. Requienid and petalodontid rudists colonized the reef as it grew upwards into their preferred water depth and environmental conditions (Scott, 1984). These rudists were successful in this facies but did not achieve total dominance; instead they are heterogeneously distributed across the reef as solitary individuals, small clusters, and densely packed colonies that grew at a sub-meter scale. This heterogeneous distribution can be problematic for facies composition assessments at a small scale, as shown in Figure 10. Here, the rudist-coral boundstone facies is not split out into multiple facies based on relative abundance of corals and rudists because mapping as such yields an extremely sporadic distribution of facies, no clear trend explaining distribution of the different reef constituents or preference for certain microhabitats, and no growth patterns that could indicate that temporal boundaries were being crossed. Heterogeneity is well-documented in modern reefs and is a source of error in small-scale population analyses that must be accounted for when diverse biota are present (Link et al., 1994; Mapstone et al., 1998). Therefore, it is more logical to conclude that organisms in Cretaceous reefs such as Paul Spur were simply heterogeneously distributed as in modern reefs.

The reappearance of the *Orbitolina* mud-dominated packstone above the rudist-coral boundstone (Fig.18F) suggests an episode of relative sea level rise and drowning of reef buildups. It can only be seen reliably in one place in outcrop, as it is thin (<30 cm thick) on the top of the reef and weathers recessively. Here, we have interpreted this event as an abrupt flooding cycle in which productive reef growth shut off and open marine sediments buried the reef, filling gaps between reef buildups and draping over existing topography. Shut-off of reef growth and the deposition of the *Orbitolina* mud-dominated packstone is attributed to increasing water depths rather than any major perturbation caused by a shift in ocean water chemistry because the unit is predominantly composed of fine carbonate mud, which is both indicative of ongoing carbonate production (despite cessation

of reef growth) and of a return to deeper, quieter waters rather than continued shallowing upwards into a more wave-dominated regime in which fine sediment would be winnowed out. Although this unit is not well exposed in outcrop between patch reefs, it may have filled the space between the tall diverse coral framestone buildup on the south side of the outcrop and the laterally extensive rudist-coral boundstone to the north, as shown in Figure 5. After lithification and subsequent uplift and exposure, it would have quickly eroded off the top of the outcrop, leaving behind the better-cemented reef exposures and the topography observed today.

The termination of the *Orbitolina* mud-dominated packstone and the re-initiation of reef growth is interpreted to represent a return to more optimal reef growth conditions, likely by another period of shallowing. This phase of reef growth is limited as in the initial first stage of reef growth at the base of the outcrop (i.e. Fig. 18B). Laterally extensive buildups with low vertical profile are replaced by smaller diameter buildups with taller profiles. Coarse-grained matrix occurs at higher concentrations than in the older reefs, and platy corals (*Microsolena*) appear small, thin, and cup-shaped, indicating that growing conditions may have been more stressed. This same relationship is seen in small reef growths observed in the skeletal grain-dominated packstone tails on the leeward side of larger reef buildups lower in the section; it is possible that sedimentation rates were higher than optimal for coral growth, leading to lower substrate colonization and a preference for growing upwards into the water column.

Following transgression and deposition of the *Orbitolina* mud-dominated packstone, reef growth began again but with much less significant buildups (Fig. 18G). *Microsolena*-dominated microbial-coral and diverse microbial-coral framestones appeared in limited pinnacle-like reefs, attaining somewhat substantial vertical growth (<3 m) but not spreading out laterally as before. The final stage of "reef" accumulation, the rudist

floatstone, fills in the space around these buildups and drapes across the older reef topography, building a deposit up to 4.4 m thick.

The rudist floatstone facies is strongly grain-dominated (75.7% matrix) and does not contain a coral framework of any kind. Instead, a diverse assemblage of rudists floats in the coarse grain-dominated packstone matrix. The diversity of rudists is in itself intriguing, as a variety of different growth forms and sizes indicative of different environments are all found together in close association. *Monopleura*, which is a small (<8 cm tall) elevator rudist, occurs commonly in small clusters on the southernmost hill of the study area. These rudists are typically found in quiet back reef or reef flank environments (Perkins, 1974; Scott, 1981, 1990), yet here they are found with petalodontids and caprinids, which are commonly attributed to higher-energy reef core and flank environments (Kerans, 2002; Perkins, 1974; Ross and Skelton, 1993). Large elevator radiolitids are also present, though in low abundances. Most rudists are *in situ* or have been toppled but not transported far from their original location. This facies therefore may initially give the appearance of a "rudist reef" that has developed without a supporting coral framework. Nevertheless, the high amount of sediment and the presence of typically more back reef protected-water rudists indicates that this facies likely developed in the energy shadow of a larger buildup further seaward (south) that acted as the sediment source and barrier creating an ideal environment for rudist growth. Rather than actively building topography, sediment and rudists simply draped over the underlying older reefs, accumulating a significant vertical buildup over time. The rudist debris rudstone deposited in a flanking debris tail on the leeward side of the northern end of the buildup is indicative of further sediment transport off-reef to the north.

High sedimentation rates derived from the breakdown and wash-over of the seaward buildup would have prevented corals from gaining a foothold during deposition

of the rudist floatstone unit. In contrast, this type of environment may have been optimal for rudist habitation, as many members of this group flourish in grain-rich deposits, preferring to support themselves by nestling into the sediment (Gili et al., 1995a, 1995b). It is unclear why rudists did not proliferate into dense colonies as seen in other Cretaceous rudist reef outcrops, such as those seen in the time equivalent Glen Rose Formation (Perkins, 1974) and at other Mural Limestone outcrops within the Bisbee Basin (e.g. Aisner, 2010; Hartshorne, 1989). Environmental conditions may not have been optimal for the growth of larger bodied rudists or vast colonies. Despite being in a protected back reef area, the energy levels in the platform interior may have still been too high for this kind of accumulation (Ross and Skelton, 1993; Scott et al., 1990); other factors such as nutrient availability, salinity, and water temperature may also have limited growth.

Chapter 6: Discussion

New interpretations of Paul Spur North

Based on the morphology and biotic composition of the reefs described here, local sea level and sedimentation rates were the two main environmental factors impacting reef growth. Platy corals colonized the deeper waters of the platform, while an abundance of diverse corals grew in slightly shallower depths. Rudists did not proliferate at depth and were uncommon to rare, but increased in abundance as shallowing occurred. Shallowing was also associated with an increase in sedimentation rate, which initially limited growth of corals spatially. Towards the end of observable reef growth at Paul Spur, high amounts of sediment accumulation eliminated coral growth entirely; corals may also have declined due to unfavorable conditions related to increased turbidity, temperatures, and salinity with additional shallowing on the platform.

Previous models of the patch reef at Paul Spur (e.g. Scott and Brenckle, 1977; Roybal, 1981; Aisner, 2010) presented a somewhat simplified view of the true depositional history of the reef. More detailed mapping of both the facies and major faults has revealed a more complex story than previously recognized. Not only does facies offset occurring solely as a result of faulting have to be considered, but multiple stages of growth must also be differentiated to successfully unravel the history of the reef. The new depositional and stratigraphic model for Paul Spur presented here adds a temporal component that clearly shows the evolution of the reef complex through time, and provides supporting evidence for sea level and sedimentation rate as the primary mechanisms mediating biotic community turnover. Additionally, standard reef biotic zonation is not as strong of a factor influencing community distribution as previously modeled (e.g. Roybal, 1981). While the back reef community can still be differentiated due to its graininess, the presence of reef rubble, and paucity of coral growth, the forereef and climax framework communities

within a single buildup are not significantly different. This is consistent with coral zonation in modern platform interior patch reefs of this scale, which are also more controlled by water depth and sedimentation than by windward-leeward zonation (e.g. Bonem and Stanley, 1977; Burke et al., 1998; Huston, 1985; Wallace and Schafersman, 1977). Investigation of other previously studied Cretaceous patch reef localities could yield insight into zonation not related to water depth.

Although initial mapping of the exposed top surface of the reef seemed to indicate substantial variation in reef facies both laterally and in a windward-leeward orientation, integrated reef stratigraphy mapped in the exposed cross-sectional view of the reef now makes it clear that the exposed top surface actually reflects multiple stages of reef growth with original topography being affected by erosion and faulting. Facies variability is also an issue, as reef frameworks are difficult to quantitatively constrain because of the size and heterogeneous distribution of reef constituents (see Fig. 10, especially in coral-rudist boundstone facies). If this outcrop were described using only cores rather than comprehensive mapping, the interpretation would likely be drastically different, especially when going through the rudist-coral boundstone facies. If the core happened to slice through one of the dense colonies of rudists within the facies, it may be interpreted as a widespread rudist reef when that is not the case. This observation should serve as a warning for those describing reef buildups with a limited amount of data: interpretations made on small-scale changes rather than large-scale trends could depict its depositional history and architecture erroneously.

Compounding the problem of facies interplay are the skeletal grain-dominated packstones, which are compositionally identical or nearly identical even when they are non-contemporaneous in deposition. In outcrop, grain-dominated packstone is found as a thick, laterally continuous shoal acting as the initiation point for the start of reef growth, as

sediment tails on the leeward side of reef buildups, and as a later generation burying later stage reefs. Presence of coral rubble assists in differentiating the "first" grain-dominated packstone from later reef-associated grain-dominated packstones, but these different units are difficult to distinguish from one another. This study therefore highlights the need to integrate rigorous three-dimensional work where possible to aid in resolving reef growth history.

CORAL-RUDIST INTERACTIONS AND POTENTIAL FOR COMPETITION

The rudist-coral reef buildups provide an opportunity to test the hypothesis of direct coral-rudist competition established by Kauffman and Johnson (1988) as a factor influencing faunal turnover in the reef ecology through time. Assessing evidence of direct competition can be difficult due to the constraints of the fossil record. Relationships are sometimes obscured from view in outcrop when matrix filling the area around the organisms of interest does not erode. Additionally, fossils found in close association may not have necessarily lived at the same time, and thus may not have interacted at all; this is especially important to consider for a complex framework structure such as a coral reef, which provides substrate for colonization even after the reef organisms have died. Nevertheless, several indications of competition described by Kauffman and Johnson (1988) can potentially be observed in outcrop, including: development of defense structures, overgrowth of competing organisms, and support of dense clusters to the exclusion of the other organism.

Defense structures would likely only be observable in rudists due to corals' reliance on cnidocytes for protection (e.g. Chornesky, 1983; Richardson et al., 1979). Rudist defense structures could manifest in features such as excessively thickened shells, spikes, and protuberances that could hold corals at a distance. Kauffman and Johnson (1988) noted

the development of rudists with spiked shells, though they interpreted the spikes as a method of stabilization via intermeshing with other nearby rudists. Götz (2003) also described balcony-like protuberances on the shells of rudists associated with nearby corals. Nevertheless, no such structures were found in any rudists at Paul Spur, despite frequent close associations between coral and rudist bodies (Figs. 16, 17). No morphological adaptations were observed in rudists; thus, it can be concluded that this method of competition does not occur.

Overgrowth relationships, if consistent (e.g. corals only growing over rudists, or rudists only growing over corals), could represent competition for light or nutrients; this competitive strategy can be observed in modern corals competing for light (Karlson, 1999). Although it is not known whether or not rudists were photosymbiotic, it has been suggested that symbiosis was a means of increasing competitiveness with corals (Kauffman and Johnson, 1988; Kauffman and Sohl, 1974; Vogel, 1975). Even if rudists did not need light to grow, the overprint relationship could still be viewed as competition for optimal habitat in more open waters, a necessity for food acquisition. At Paul Spur, both types of overgrowth relationships (corals growing on rudists and rudists growing on corals) were observed (Figs. 16, 17). Corals more frequently overgrew rudists, which could potentially indicate that corals were actually better adapted for this sort of competition, which directly opposes the hypothesis of rudist reef dominance through competition. Nevertheless, these overgrowth relationships were infrequent and inconsistent enough that definitive conclusions about direct competition between corals and rudists cannot be drawn; they can only provide evidence against competition as a primary component of rudist dominance over corals.

Dense clusters of organisms could work to exclude a competitor from an optimal habitat. Although some rudists such as toucasids frequently occur in tightly packed

monospecific clusters, this community typically occurs in very muddy areas that corals would be unlikely to colonize anyways. Therefore, this relationship as evidence of competition has been excluded to avoid potential confounding factors.

In summary, the community interactions observed in the rudist-coral reefs provide limited (if any) support for the competition hypothesis. Overall trends in reef development, composition, and morphology are much more strongly indicative of environmental controls on faunal turnover.

COMPARISON OF QUANTITATIVE ECOLOGICAL METHODOLOGIES

One of the goals of this research was to assess quantitative techniques for assessing reef facies composition. Specifically, the two facies composition analysis techniques compared were random point counting of a selected sample area (following Hamon et al., 2016) and comprehensive mapping of the selected area via a digitized image. Prior work by Bernecker et al. (1999) compared various reef sampling methodologies and concluded that outcrop photography was unreliable for differentiation of reef fabrics; however, modern photography equipment has substantially improved with regard to image quality and resolution since then and thus the technique merited reassessment. Facies composition analysis of Mural patch reefs has been conducted in the field in the past (e.g. Hartshorne, 1989; Roybal, 1981). This technique involves point counting at regular predetermined intersections within a selected area; it can be time consuming in the field and can even be impossible in some circumstances depending on outcrop conditions. Photographing a sample area thoroughly and compiling it into a digitized, undistorted sample can reduce the amount of valuable field time used for facies analysis. The sample image can be loaded into a point counter program (such as JMicrovision, as used in this study) that allows quicker and potentially more accurate analysis. To test the accuracy of the analysis,

selected samples were both annotated (colored over by hand) and point counted. The two techniques were found to yield similar results to one another for reef framework facies, coming within 5% accuracy of one another for all reef constituents (Appendix B). However, the same was not true for the grain-dominated rudist floatstone facies. While "reef constituents" (rudists) still came within 6% of one another for annotation and point count analyses, large rudists were consistently overrepresented by point counting, while matrix and small rudists were underrepresented. This effect is attributed to the discrepancy in relative skeletal grain size (see Jacobson et al., 2011), as large-bodied requienids and caprinids are often counted more than once during point counting while smaller or less abundant skeletal grains may be skipped over entirely. Increasing the number of point counts from 250 to 500 reduces this effect. Therefore, care must be taken when utilizing point counting for facies analysis, especially in more grain-dominated facies where sampling error is more likely; using annotation to verify the accuracy of point counting is a good strategy to reduce error, although time consuming.

BROADER APPLICATIONS AND IMPLICATIONS

From a broader perspective, this study resolves some anomalies that previously made Paul Spur an oddity in the context of other Cretaceous reefs as well as modern patch reefs. By integrating a temporal component into the interpretation of the reef's history, the apparently strong biotic zonation, which would not typically occur in a small-scale, shallow water platform interior patch reef, is instead shown to be a result of different generations of reef growth (i.e. Fig. 18). Reef buildups are mostly composed of one community, though different reef constituents may be heterogeneously distributed, and may be associated with a grain-rich tail in which smaller reef buildups and more fragile sheltered reef organisms grew. These tails seem to develop more preferentially during periods when reefs are

affected by strong wave action, either when they grow up into fair weather wave base or when sea level drops.

The new depositional/stratigraphic model for Paul Spur may have implications for those interested in patch reefs as hydrocarbon sources in the subsurface. Previous work at Paul Spur has identified it as an excellent outcrop analog for the patch reefs of the Lower Glen Rose Formation (Aisner, 2010); it may also be closely analogous to reefs in the James Limestone (Achauer and Johnson, 1969) and the Rodessa Formation (Scott, 1990). Patch reefs in the Glen Rose developed in moderately shallow water on the distally steepened ramp of the passive margin of what is now the Gulf of Mexico in the early Albian recovery period following OAE 1b (Phelps et al., 2014, 2015). Earlier coral-rudist "reefs" (more accurately labeled as bafflestone biostromes) in this formation did not have significant depositional relief; however, later caprinid-dominated assemblages grew up to 10 m of relief (Scott et al., 2007). Despite the differences in faunal assemblages between Glen Rose reefs and Paul Spur, these reefs exhibit a similar asymmetric morphology driven by windward-leeward currents and wave action (Aconcha, 2008). Notably, they altered shape during different periods of growth based on sea level fluctuations, which is also now demonstrated at Paul Spur. The Glen Rose patch reefs were also associated with *Orbitolina*-peloid packstones that are likely correlative in depositional setting to the *Orbitolina* mud-dominated packstones observed at Paul Spur, providing further evidence for similarities in depositional environment and development.

Paul Spur is likely another reef representative of post-OAE carbonate platform recovery. Previous work has associated the *Orbitolina* packstone with transgression and flooding caused by the drowning of the Comanche platform after OAE 1b, and has posited that it represents an environmentally stressed assemblage as it is primarily dominated by one orbitolinid species (*O. texana)* (Phelps et al., 2014, 2015). The re-initiation of reef

growth in the form of patch reefs represents recovery from a stressed to a healthy carbonate system (Phelps et al., 2015). At Paul Spur, *Microsolena* and its associated stromatolitic microbial mats are the pioneer community. The presence of only one type of coral may be indicative simply of deeper waters, as suggested by others (Achauer and Johnson, 1969; Bebout and Loucks, 1974; Greenberg, 1986; Scott, 1990, 1995); however, the possibility of the facies as the representative initiation of the recovery phase, with only one coral able to withstand ocean conditions at that time well enough to flourish, should not be ruled out. The subsequent diversification of the coral assemblage in the second stage of growth is likely not only related to fluctuations in sea level, but to biotic recovery as well. As environmental conditions improved for growth of less-hardy aragonitic organisms, other corals would be able to colonize the reef, leading to the more diverse assemblage observed in the second stage of reef growth. It should be noted though that though recovery likely plays a part in the biotic composition of the reefs at Paul Spur, eustatic fluctuations and variable sedimentation rates were the main drivers of reef development and growth from an architectural perspective.

Loucks and Kerans (2003) identified the patch reefs and associated grainy tails of the Glen Rose Formation as potential hydrocarbon targets with moderate reservoir quality, depending on the preservation of porosity; it is therefore useful to know what reef geometries and depositional environments to look for when identifying these units. Recognizing the importance of sea level and sedimentation rates controlling reef architecture aids in hypothesizing geometries and targeting areas of interest when only 1D or 2D data are available (e.g. seismic or cores), provided that the data are placed in a stratigraphic framework that has been well resolved. What is now known about Paul Spur could be directly applied to these different reef growth strategies observed in the subsurface Glen Rose for improved identification of ideal targets. Rather than extrapolating a generic

domed reef shape for subsurface patch reefs, reef architecture can be more accurately modeled using facies data with environmental context applied, as seen in the stratigraphic model of Paul Spur.

Chapter 7: Conclusions

The degree of exposure and quality of preservation of reefs at Paul Spur makes it exceptionally well suited for comprehensive facies and stratigraphic analysis. Here, the addition of new high-resolution facies mapping to a three-dimensional outcrop model facilitates reconstruction of the depositional history of the reef. Local sea level and sedimentation rates control the growth and architecture of multiple generations of reefs and reflect an overall shallowing upwards sequence. The deeper water *Microsolena*-dominated microbial coral framestone builds the initial pioneer reef on top of a low-relief abraded *Orbitolina* skeletal grain-dominated packstone shoal. A more diverse coral assemblage follows in the second period of growth; the introduction of rudists to the diverse coral framestone marks the third transition as shallowing continues. A brief transgression precedes a drastic regime change and the subsequent deposition of the rudist floatstone, which is composed of a much higher percentage of matrix than previous reef facies and is indicative of high sediment supply likely sourced from a more seaward reef buildup.

Ecological succession and community evolution are important elements contributing to the shape and extent of the reefs. The paleoecology of each stage of growth is closely tied to water depth and sedimentation, emphasizing the importance of the interplay of biotic and abiotic controls on reef development. Initial reef growth and coral assemblage diversification may also be related to recovery of the carbonate system following OAE 1b. Corals and rudists are found to be noncompetitive with each other and changing population sizes, with increasing numbers of rudists and decreasing numbers of corals through time, are more likely to reflect evolving environmental conditions.

The revised interpretation of the history of reef growth at Paul Spur highlights the utility of modern high-resolution and digital data gathering techniques for improved

stratigraphic analysis. This new model and associated data can be applied to problems in the subsurface with respect to patch reef geometries and facies relationships, which will improve confidence in targeting potential reservoirs in future petroleum exploration.

Appendix A

This appendix includes all rock specimens and thin sections figured within this text. It includes the facies represented, a brief description of the rock, and geographic location data if applicable.

Sample ID	Sample Type	Facies	Brief Description	Collection Information
PS-A1	Hand sample, slabbed	1	*Orbitolina* mud-dominated packstone facies sample with visible *Orbitolina*	31.38889°, -109.7575°
PS-A1-A-TS	Thin section	1	Thin section of *Orbitolina* mud-dominated packstone facies with abundant *Orbitolina* in a fine skeletal mud-dominated packstone matrix	31.38889°, -109.7575°
PS-A2	Hand sample, slabbed	2	Skeletal grain-dominated packstone facies sample with visible coarse skeletal (predominantly molluscan) grains	31.3873°, -109.7565°
PS-A2-A-TS	Thin section	2	Thin section of lower skeletal grain-dominated packstone facies showing large abraded skeletal grains and rounded *Orbitolina*	31.3873°, -109.7565°
PS-A9	Hand sample, slabbed and polished	3	Sample of *Microsolena* -dominated microbial-coral framestone facies showing the relationship between a thin platy *Microsolena* coral and a stromatolitic microbial mat growing on top, with matrix filling in top surface over microbial mat	Float
PS-A9-A-TS	Thin section	3	Thin section from sample PS-A9 demonstrating fine skeletal mud-dominated packstone draping across and filling digitate top surface of microbial mat	Float
PS-A9-C-TS	Thin section	3	Thin section from sample PS-A9 comprised of bored *Microsolena* (white), with encrusting algae (arrow) and stromatolitic microbial mat with laminar texture growing on top of coral	Float

Appendix B

This appendix includes the facies composition analysis data for all measured quadrats at Paul Spur.

			GPS Data		Coral Types			Rudist Types				Matrix Types		Summary Categories			
Quad #	Facies ID	Quadrat Orientation	Latitude	Longitude	Microsolena	Branching Coral	Coral Misc	Microbial	Caprinid	Requieniid / Petalodontid	Rudist Misc.	*Monopleura*	Fine mud	Skeletal GDP	Sum Coral	Sum Microbial	Sum Rudist	Sum Matrix
1	M FRS	Cross-section	31.38577	-109.755264	32.8%	0.0%	0.0%	18.4%	1.6%	0.0%	0.0%	0.0%	18.0%	29.2%	32.8%	18.4%	1.6%	47.2%
2	CR BS	Cross-section	-	-	19.0%	10.5%	17.0%	7.0%	0.0%	1.0%	0.0%	0.0%	15.0%	30.5%	46.5%	7.0%	1.0%	45.5%
3	DC FRS	Cross-section	31.38574	-109.755452	20.0%	16.0%	18.5%	5.0%	3.0%	0.0%	0.5%	0.0%	12.5%	24.5%	54.5%	5.0%	3.5%	37.0%
4	DC FRS	Cross-section	31.38574	-109.755452	15.5%	28.0%	14.0%	2.0%	0.5%	0.0%	0.0%	0.0%	13.5%	26.5%	57.5%	2.0%	0.5%	40.0%
5	DC FRS	Cross-section	31.38574	-109.755452	-	-	-	-	-	-	-	-	-	-	-	-	-	-
6	CR BS	Cross-section	-	-	1.6%	1.2%	3.2%	0.4%	2.4%	17.2%	2.0%	0.0%	16.0%	56.0%	6.0%	0.4%	21.6%	72.0%
7	R RS	Cross-section	31.38564	-109.756106	0.0%	0.0%	6.0%	0.0%	8.4%	4.8%	1.6%	0.8%	0.0%	78.4%	6.0%	0.0%	15.6%	78.4%
8	CR BS	Cross-section	31.38559	-109.756288	6.8%	0.0%	23.6%	0.0%	1.2%	5.6%	0.4%	0.0%	3.2%	59.2%	30.4%	0.0%	7.2%	62.4%
9	CR BS	Plan	31.38554	-109.756359	1.2%	4.0%	12.0%	0.4%	0.4%	3.6%	2.8%	2.0%	3.6%	70.0%	17.2%	0.4%	8.8%	73.6%
10	R RS	Cross-section	31.38541	-109.75582	0.0%	0.0%	1.5%	0.0%	0.0%	9.0%	3.0%	1.0%	0.0%	85.5%	1.5%	0.0%	13.0%	85.5%
11	R RS	Cross-section	31.38591	-109.756137	0.0%	0.0%	5.0%	0.0%	4.0%	15.0%	1.5%	0.0%	0.0%	74.5%	5.0%	0.0%	20.5%	74.5%
12	R RS	Plan	31.38591	-109.755902	0.0%	0.0%	4.5%	0.0%	3.5%	18.0%	0.5%	2.0%	0.0%	71.5%	4.5%	0.0%	24.0%	71.5%
13	R RS	Plan	31.38591	-109.755902	0.0%	0.0%	4.0%	0.0%	2.8%	18.8%	2.4%	0.0%	0.0%	72.0%	4.0%	0.0%	24.0%	72.0%
14	CR BS	Cross-section	31.38596	-109.755642	8.4%	4.4%	20.0%	6.0%	4.0%	1.2%	4.4%	0.0%	16.0%	35.6%	32.8%	6.0%	9.6%	51.6%
15	DC FRS	Plan	31.3864	-109.756312	2.8%	18.0%	34.8%	0.0%	0.8%	0.0%	0.0%	0.0%	2.4%	41.2%	55.6%	0.0%	0.8%	43.6%
16	M FRS	Cross-section	-	-	41.2%	0.0%	2.4%	16.8%	0.0%	0.0%	0.0%	0.0%	10.8%	28.4%	43.6%	16.8%	0.0%	39.2%
17	DC FRS	Plan	31.38676	-109.7566	39.6%	2.8%	10.4%	4.8%	0.0%	0.0%	0.0%	0.0%	18.0%	24.4%	52.8%	4.8%	0.0%	42.4%
18	CR BS	Cross-section	31.38678	-109.757175	0.0%	0.0%	2.0%	0.0%	10.0%	24.4%	4.4%	0.0%	2.8%	56.4%	2.0%	0.0%	38.8%	59.2%
19	DC FRS	Cross-section	31.38716	-109.756975	28.8%	10.0%	7.2%	6.8%	0.4%	0.0%	0.0%	0.0%	20.0%	26.8%	46.0%	6.8%	0.4%	46.8%
20	RD RS	Plan	31.38774	-109.756846	0.0%	0.0%	1.6%	0.0%	31.2%	17.6%	4.8%	0.0%	14.8%	30.0%	1.6%	0.0%	53.6%	44.8%
21	RD RS	Cross-section	31.38786	-109.756759	0.0%	0.0%	1.2%	0.0%	30.4%	23.2%	7.2%	0.0%	19.6%	18.4%	1.2%	0.0%	60.8%	38.0%
22	RD RS	Cross-section	31.38786	-109.756759	0.0%	0.0%	0.4%	0.0%	28.8%	23.2%	10.8%	0.0%	26.0%	10.8%	0.4%	0.0%	62.8%	36.8%
23	RD RS	Cross-section	-	-	0.0%	0.0%	1.6%	0.0%	19.2%	29.2%	7.2%	0.0%	37.2%	5.6%	1.6%	0.0%	55.6%	42.8%
24	M FRS	Cross-section	31.38771	-109.756639	30.8%	4.0%	6.0%	9.6%	0.4%	0.0%	0.8%	0.0%	20.8%	27.6%	40.8%	9.6%	1.2%	48.4%
25	CR BS	Cross-section	31.38778	-109.756982	24.0%	2.0%	14.8%	11.6%	3.2%	10.4%	0.0%	0.0%	18.8%	14.4%	40.8%	11.6%	13.6%	33.2%
26	M FRS	Cross-section	-	-	42.0%	0.0%	2.8%	11.6%	0.0%	0.0%	0.0%	0.0%	22.0%	21.6%	44.8%	11.6%	0.0%	43.6%
27	M FRS	Cross-section	31.38943	-109.757953	26.8%	0.0%	1.6%	18.4%	0.0%	0.0%	0.0%	0.0%	0.0%	52.8%	28.4%	18.4%	0.0%	52.8%
28	CR BS	Cross-section	31.38655	-109.757685	1.6%	38.0%	17.2%	0.4%	0.8%	4.0%	0.0%	0.0%	18.8%	19.2%	56.8%	0.4%	4.8%	38.0%
29	CR BS	Cross-section	31.38692	-109.757821	0.0%	0.0%	6.4%	0.0%	8.8%	32.4%	5.6%	0.0%	33.6%	13.2%	6.4%	0.0%	46.8%	46.8%
30	DC FRS	Cross-section	31.38723	-109.757617	24.0%	12.4%	7.2%	14.0%	0.8%	0.8%	0.0%	0.0%	21.2%	19.6%	43.6%	14.0%	1.6%	40.8%

Appendix C

This appendix compares point counting and annotation techniques for selected quadrats for each described reef facies.

ID: Q1 M FRS	Microsolena	Massive / Misc. Corals	Branching Coral	Microbial Growth	Matrix	Caprinid	Requienid / Petalodontid	Other rudist	*Monopleura*	Total Coral	Total Microbial	Total Rudist	Total Matrix
Point Ct.	32.80%	0.00%	0.00%	18.40%	47.20%	1.60%	0.00%	0.00%	0.00%	32.8%	18.4%	1.6%	47.2%
Annotate	28.70%	0.00%	0.00%	15.90%	53.85%	1.60%	0.00%	0.00%	0.00%	28.7%	15.9%	1.6%	53.8%
Difference	-4.10%	0.00%	0.00%	-2.50%	6.65%	0.00%	0.00%	0.00%	0.00%	-4.1%	-2.5%	0.0%	6.6%

ID: Q19 DC FRS	Microsolena	Massive / Misc. Corals	Branching Coral	Microbial Growth	Matrix	Caprinid	Requienid / Petalodontid	Other rudist	*Monopleura*	Total Coral	Total Microbial	Total Rudist	Total Matrix
Point Ct.	28.80%	7.20%	10.00%	6.80%	46.80%	0.04%	0.00%	0.00%	0.00%	46.00%	6.80%	0.40%	46.80%
Annotate	29.43%	5.85%	6.44%	5.86%	52.20%	0.22%	0.00%	0.00%	0.00%	41.80%	5.86%	0.20%	52.33%
Difference	0.63%	-1.35%	-3.56%	-0.94%	5.40%	0.18%	0.00%	0.00%	0.00%	-4.20%	-0.94%	-0.20%	5.53%

ID: Q28 CR BS	Microsolena	Massive / Misc. Corals	Branching Coral	Microbial Growth	Matrix	Caprinid	Requienid / Petalodontid	Other rudist	*Monopleura*	Total Coral	Total Microbial	Total Rudist	Total Matrix
Point Ct.	1.60%	17.20%	38.00%	0.40%	38.00%	0.80%	4.00%	0.00%	0.00%	56.80%	0.40%	4.80%	38.00%
Annotate	0.79%	17.84%	33.88%	0.00%	44.86%	0.42%	2.82%	0.00%	0.00%	52.51%	0.00%	3.24%	44.86%
Difference	-0.81%	0.64%	-4.12%	-0.40%	6.86%	-0.38%	-1.18%	0.00%	0.00%	-4.29%	-0.40%	-1.56%	6.86%

ID: Q11 R RS	Microsolena	Massive / Misc. Corals	Branching Coral	Microbial Growth	Matrix	Caprinid	Requienid / Petalodontid	Other rudist	*Monopleura*	Total Coral	Total Microbial	Total Rudist	Total Matrix
Point Ct.	0.00%	5.00%	0.00%	0.00%	74.50%	4.00%	15.00%	1.50%	0.00%	5.00%	0.00%	20.50%	74.50%
Annotate	0.00%	2.03%	0.00%	0.00%	85.89%	1.10%	9.40%	1.66%	0.04%	2.03%	0.00%	12.20%	85.79%
Difference	0.00%	-2.97%	0.00%	0.00%	11.39%	-2.90%	-5.60%	0.16%	0.04%	-2.97%	0.00%	-8.30%	11.29%

ID: Q22 RD RS	Microsolena	Massive / Misc. Corals	Branching Coral	Microbial Growth	Matrix	Caprinid	Requienid / Petalodontid	Other rudist	*Monopleura*	Total Coral	Total Microbial	Total Rudist	Total Matrix
Point Ct.	0.00%	0.40%	0.00%	0.00%	36.80%	28.80%	23.20%	10.80%	0.00%	0.40%	0.00%	62.80%	36.80%
Annotate	0.00%	0.09%	0.00%	0.00%	46.50%	24.44%	20.45%	8.82%	0.00%	0.08%	0.00%	53.71%	46.50%
Difference	0.00%	-0.31%	0.00%	0.00%	9.70%	-4.36%	-2.75%	-1.98%	0.00%	-0.32%	0.00%	-9.09%	9.70%

References

Achauer, C.W., Johnson, H., 1969. Algal stromatolites in the James Reef Complex (Lower Cretaceous), Fairway Field, Texas. J. Sediment. Petrol. 39, 1466–1472. doi:10.1306/74D71E5B-2B21-11D7-8648000102C1865D

Aconcha, E.S., 2008. Integrated core, well log, and seismic interpretation of Albian patch reefs in Maverick Basin, SW Texas. University of Texas at Austin.

Aisner, R.E., 2010. Patch-reef and ramp interior facies architecture of the Early Albian Mural Limestone, Southeastern Arizona. University of Texas at Austin.

Bebout, D.G., Loucks, R.G., 1974. Stuart City Trend, Lower Cretaceous, South Texas: a carbonate shelf-margin model for hydrocarbon exploration.

Bernecker, M., Weidlich, O., Flügel, E., 1999. Response of Triassic reef coral communities to sea-level fluctuations, storms and sedimentation: Evidence from a spectacular outcrop (Adnet, Austria). Facies 40, 229–280. doi:10.1007/BF02537476

Bonem, R.M., Stanley, G.D., 1977. Zonation of a lagoonal patch reef: analysis, comparison, and implications for fossil biohermal assemblages, in: Proceedings, Third International Coral Reef Symposium. Rosenstiel School of Marine and Atmospheric Science, Miami, Florida, pp. 175–181.

Burke, C.D., McHenry, T.M., Bischoff, W.D., Mazzullo, S.J., 1998. Coral diversity and mode of growth of lateral expansion patch reefs at Mexico Rocks, northern Belize shelf, Central America. Carbonates and Evaporites 13, 32–42. doi:10.1007/BF03175432

Chornesky, E.A., 1983. Induced development of sweeper tentacles on the reef coral *Agaricia agaricites*: a response to direct competition. Biol. Bull. 165, 569–581.

Embry, A.F., Klovan, J.E., 1971. A Late Devonian reef tract on Northeastern Banks Island, N.W.T. Bull. Can. Pet. Geol. 19, 730–781.

Fricke, H.W., Schuhmacher, H., 1983. The depth limits of Red Sea stony corals: an ecophysiological problem (a deep diving survey by submersible). Mar. Ecol. 4, 163–194. doi:10.1111/j.1439-0485.1983.tb00294.x

Gili, E., Masse, J.-P., Skelton, P.W., 1995a. Rudists as gregarious sediment-dwellers, not reef-builders, on Cretaceous carbonate platforms. Palaeogeogr. Palaeoclimatol. Palaeoecol. 118, 245–267. doi:10.1016/0031-0182(95)00006-X

Gili, E., Skelton, P.W., Vicens, E., Obrador, A., 1995b. Corals to rudists—an environmentally induced assemblage succession. Palaeogeogr. Palaeoclimatol. Palaeoecol. 119, 127–136. doi:10.1016/0031-0182(95)00064-X

Gonzalez-Leon, C.M., Scott, R.W., Löser, H., Lawton, T.F., Robert, E., Valencia, V.A., 2008. Upper Aptian-Lower Albian Mural Formation: stratigraphy, biostratigraphy

and depositional cycles on the Sonoran shelf, northern México. Cretac. Res. 29, 249–266. doi: 10.1016/j.cretres.2007.06.001

Götz, S., 2003. Biotic interaction and synecology in a Late Cretaceous coral-rudist biostrome of southeastern Spain. Palaeogeogr. Palaeoclimatol. Palaeoecol. 193, 125–138. doi:10.1016/S0031-0182(02)00719-8

Greenberg, J.G., 1986. Diagenesis of the Lower Cretaceous James Limestone, Fairway Field, east Texas: a petrographic and geochemical study. University of Texas at Austin.

Hamon, Y., Deschamps, R., Joseph, P., Doligez, B., Schmitz, J., Lerat, O., 2016. Integrated workflow for characterizing and modeling a mixed sedimentary system: The Ilerdian Alveolina Limestone Formation (Graus – Tremp Basin, Spain). Comptes Rendus Geosci. 348, 520–530. doi:10.1016/j.crte.2015.07.002

Hartshorne, P.M., 1989. Facies architecture of a Lower Cretaceous coral-rudist patch reef, Arizona. Cretac. Res. 10, 311–336. doi:10.1016/0195-6671(89)90008-6

Hayes, P.T., 1970. Cretaceous paleogeography of southeastern Arizona and adjacent areas. U.S. Geol. Surv. Prof. Pap. 658-B 1–42.

Hofker, J., 1963. Studies on the genus *Orbitolina* (Foraminiferida). Leidse Geol. Meded. 29, 181–253.

Huston, M.A., 1985. Patterns of species diversity on coral reefs. Annu. Rev. Ecol. Syst. 16, 149–177. doi:10.1146/annurev.es.16.110185.001053

Jacobsen, N.D., Twitchett, R.J., Krystyn, L., 2011. Palaeoecological methods for assessing marine ecosystem recovery following the Late Permian mass extinction event. Palaeogeogr. Palaeoclimatol. Palaeoecol. 308, 200–212. doi:10.1016/j.palaeo.2010.04.024

Jenkyns, H.C., 1980. Cretaceous anoxic events: from continents to oceans. J. Geol. Soc. London. 137, 171–188. doi:10.1144/gsjgs.137.2.0171

Johnson, C.C., 2002. The Rise and Fall of Rudist Reefs: Reefs of the dinosaur era were dominated not by corals but by odd mollusks, which died off at the end of the Cretaceous from causes yet to be discovered. Am. Sci. 90, 148–153.

Johnson, C.C., Barron, E.J., Kauffman, E.G., Arthur, M.A., Fawcett, P.J., Yasuda, K., 1996. Middle Cretaceous reef collapse linked to ocean heat transport. Geology 24, 376–380. doi:10.1130/0091-7613(1996)024<0376

Karlson, R.H., 1999. Interspecific competition, in: Dynamics of Coral Communities. Kluwer, Dordrecht.

Kauffman, E.G., Johnson, C.C., 1988. The morphological and ecological evolution of Middle and Upper Cretaceous rudistids. Palaios 3, 194–216. doi:10.2307/3514530

Kauffman, E.G., Sohl, N.F., 1979. Rudists, in: Fairbridge, R.W., Jablonski, D. (Eds.), The Encyclopedia of Paleontology. Dowden, Hutchinson & Ross, Inc., Stroudsburg, Pennsylvania, pp. 723–736.

Kerans, C., 2002. Styles of rudist buildup development along the northern margin of the Maverick Basin, Pecos River Canyon , Southwest Texas. Gulf Coast Assoc. Geol. Soc. Trans. 52, 501–516.

Kerans, C., 2010. Barremian-Albian carbonate reservoirs, in: Reservoir Characterization Research Laboratory Annual Review Meeting Proceedings. Bureau of Economic Geology, The University of Texas at Austin, Austin, TX.

Link, W.A., Barker, R.J., Sauer, J.R., Droege, S., 1994. Errors in animal counts due to within site variability. Ecology 75, 1097–1108.

Loucks, R.G., Kerans, C., 2003. Lower Cretaceous Glen Rose "patch reef" reservoir in the Chittim Field, Maverick County, south Texas. Gulf Coast Assoc. Geol. Soc. Trans. 53, 490–503.

Mapstone, B.D., Ayling, A.M., Choat, J.H., 1998. Scales and magnitudes of variation in population densities of some coral reef organisms. Research Publication No. 49 of the Great Barrier Reef Marine Park Authority, Townsville, Queensland, Australia.

Monreal, R., 1985. Lithofacies, depositional environments, and diagenesis of the Mural Limestone (Lower Cretaceous), Lee Siding area, Cochise County, Arizona. The University of Arizona.

Neumann, A.C., Macintyre, I., 1985. Reef response to sea level rise: Keep-up, catch-up or give-up, in: Proceedings of the Fifth International Coral Reef Congress. Tahiti, pp. 105–110.

Perkins, B.F., 1962. Guide to the recognition of the rudist groups of the Gulf of Mexico and Caribbean region, EPR Report 673. ed. Shell Development Company, Houston, TX.

Perkins, B.F., 1974. Paleoecology of a rudist reef complex in the Comanche Cretaceous Glen Rose Limestone of central Texas. Geosci. Man 8, 131–174.

Phelps, R.M., Kerans, C., Loucks, R.G., Da Gama, R.O.B.P., Jeremiah, J., Hull, D., 2014. Oceanographic and eustatic control of carbonate platform evolution and sequence stratigraphy on the Cretaceous (Valanginian-Campanian) passive margin, northern Gulf of Mexico. Sedimentology 61, 461–496. doi:10.1111/sed.12062

Phelps, R.M., Kerans, C., Da-Gama, R.O.B.P., Jeremiah, J., Hull, D., Loucks, R.G., 2015. Response and recovery of the Comanche carbonate platform surrounding multiple Cretaceous oceanic anoxic events, northern Gulf of Mexico. Cretac. Res. 54, 117–144. doi:10.1016/j.cretres.2014.09.002

Pittet, B., van Buchem, F.S.P., Hillgartner, H., Razin, P., Grotsch, J., Droste, H., 2002. Ecological succession, palaeoenvironmental change, and depositional sequences of

Barremian – Aptian shallow-water carbonates in northern Oman. Sedimentology 49, 555–581. doi:10.1046/j.1365-3091.2002.00460.x

Richardson, C.A., Dustan, P., Lang, J.C., 1979. Maintenance of living space by sweeper tentacles of *Montastrea cavernosa*, a Caribbean reef coral. Mar. Biol. 55, 181–186. doi:10.1007/BF00396816

Rosen, B.R., Aillud, G.S., Bosellini, F.R., Clack, N.J., Insalaco, E., Valldeperas, F.X., Wilson, M.E.J., 2002. Platy coral assemblages: 200 million years of functional stability in response to the limiting effects of light and turbidity, in: Proceedings 9th International Coral Reef Symposium. Bali, Indonesia, p. 1.

Ross, D.J., Skelton, P.W., 1993. Rudist formations of the Cretaceous: a palaeoecological, sedimentological and stratigraphical view, in: Sedimentology Review/1. Blackwell Scientific Publications, pp. 73–91.

Roybal, G.H., 1981. Facies development in a Lower Cretaceous coral-rudist patch reef (Mural Limestone, southeast Arizona). Mt. Geol. 18, 46–56. doi:10.1016/0195-6671(89)90008-6

Schroeder, R., van Buchem, F.S.P., Cherchi, A., Baghbani, D., Vincent, B., Immenhauser, A., Granier, B., 2010. Revised orbitolinid biostratigraphic zonation for the Barremian-Aptian of the eastern Arabian Plate and implications for regional stratigraphic correlations. GeoArabia Spec. Publ. 4 1, 49–96.

Scott, R.W., 1979. Depositional model of Early Cretaceous coral-algal-rudist reefs, Arizona. Am. Assoc. Pet. Geol. Bull. 63, 1108–1127.

Scott, R.W., 1981. Biotic relations in Early Cretaceous coral-algal-rudist reefs, Arizona. J. Paleontol. 55, 463–478.

Scott, R.W., 1984. Evolution of Early Cretaceous reefs in the Gulf of Mexico. Palaeontogr. Am. 54, 406–412. doi:10.2307/3514529

Scott, R.W., 1987. Stratigraphy and correlation of the Cretaceous Mural Limestone, Arizona and Sonora., in: Dickinson, W.R., Klute, M.A. (Eds.), Mesozoic Rocks of Southern Arizona and Adjacent Areas. Arizona Geological Society Digest 18, pp. 327–334.

Scott, R.W., 1988. Evolution of Late Jurassic and Early Cretaceous reef biotas. Palaios 3, 184–193. doi:10.2307/3514529

Scott, R.W., 1990. Models and stratigraphy of mid-Cretaceous reef communities, Gulf of Mexico. Concepts in sedimentology and paleontology, v. 2. doi:10.2110/csp.90.02.0001

Scott, R.W., 1995. Global environmental controls on Cretaceous reefal ecosystems. Palaeogeogr. Palaeoclimatol. Palaeoecol. 119, 187–199. doi:10.1016/0031-0182(94)00068-9

Scott, R.W., Brenckle, P.L., 1977. Biotic zonation of a Lower Cretaceous coral-algal-rudist reef, Arizona. Proceedings, Third Int. Coral Reef Symp. 183–189.

Scott, R.W., Fernandez-Mendiola, P.A., Gili, E., Simo, A., 1990. Persistence of coral-rudist reefs into the Late Cretaceous. Palaios 5, 98–110. doi:10.2307/3514807

Scott, R.W., Filkorn, H.F., 2007. Barremian-Albian rudist zones, U.S. Gulf Coast, in: Scott, R.W. (Ed.), Cretaceous Rudists and Carbonate Platforms: Environmental Feedback. SEPM Special Publication No. 87, pp. 167–180. doi:10.2110/pec.07.87.0167

Scott, R.W., Molineux, A.M., Löser, H., Mancini, E.., 2007. Lower Albian sequence stratigraphy and coral buildups: Glen Rose Formation, Texas, U.S.A., in: Scott, R.W. (Ed.), Cretaceous Rudists and Carbonate Platforms: Environmental Feedback. SEPM Special Publication No. 87, pp. 181–191.

Scott, R.W., Warzeski, E.R., 1993. An Aptian-Albian shelf ramp, Arizona and Sonora. Am. Assoc. Pet. Geol. Mem. 56, 71–79.

Skelton, P.W., 1978. The evolution of functional design in rudists (Hippuritacea) and its taxonomic implications. Philos. Trans. R. Soc. Lond. B. Biol. Sci. 284, 305–318. doi:10.1098/rstb.1978.0069

Skelton, P.W., 2013. Rudist classification for the revised Bivalvia volumes of the "Treatise on Invertebrate Paleontology." Caribb. J. Earth Sci. 45, 9–33.

Skelton, P.W., Gili, E., 2012. Rudists and carbonate platforms in the Aptian: a case study on biotic interactions with ocean chemistry and climate. Sedimentology 59, 81–117. doi:10.1111/j.1365-3091.2011.01292.x

Vilas, L., Masse, J.P., Arias, C., 1995. *Orbitolina* episodes in carbonate platform evolution: The Early Aptian model from SE Spain. Palaeogeogr. Palaeoclimatol. Palaeoecol. 119, 35–45. doi:10.1016/0031-0182(95)00058-5

Vogel, K., 1975. Endosymbiotic algae in rudists? Palaeogeogr. Palaeoclimatol. Palaeoecol. 17, 327–332. doi:10.1017/CBO9781107415324.004

Wallace, R.J., Schafersman, S.D., 1977. Patch-reef ecology and sedimentology of Glovers Reef Atoll, Belize: modern and ancient reefs, in: Frost, S.H., Weiss, M.P., Saunders, J.B. (Eds.), Reefs and Related Carbonates. American Association of Petroleum Geologists, Studies in Geology, pp. 37–52.

Warzeski, E.R., 1987. Revised stratigraphy of the Mural Limestone: A Lower Cretaceous carbonate shelf in Arizona and Sonora, in: Dickinson, W.R., Klute, M.A. (Eds.), Mesozoic Rocks of Southern Arizona and Adjacent Areas. Arizona Geological Society Digest 18, pp. 335–363.

van der Plas, L., Tobi, A.C., 1965. A chart for judging the reliability of point counting results. Am. J. Sci. 263, 87–90. doi:10.2475/ajs.263.1.87

Zahm, C.; Lambert, J.; Kerans, C., 2016. Use of unmanned aerial vehicles (UAVs) to create digital outcrop models: An example from the Cretaceous Cow Creek Formation, Central Texas. GCAGS J. 5, 180–188.

Vita

Kelly E. Hattori is a North Carolina native who came to the University of Texas at Austin in 2015 after working for the National Park Service as a paleontology and museum technician. She graduated from the University of North Carolina at Wilmington in 2014 with a dual B.S. in Marine Biology and Geology and was originally interested in Pleistocene invertebrate paleontology. After coming to the University of Texas at Austin and getting more deeply involved with carbonate geology from a sequence stratigraphic perspective, she became interested in combining paleontology with sequence stratigraphy for better understanding of carbonate systems.

Permanent email address: kelly_hattori@nc.rr.com
This thesis was typed by the author.